Trends in the nonvolcanic component of stratospheric aerosol over the period 1971–2004

Terry Deshler,[1] Richard Anderson-Sprecher,[2] Horst Jäger,[3] John Barnes,[4] David J. Hofmann,[4] Barclay Clemesha,[5] Dale Simonich,[5] M. Osborn,[6] R. G. Grainger,[7] and Sophie Godin-Beekmann[8]

[1] The six longest records of stratospheric aerosol (in situ measurements at Laramie, Wyoming, lidar records at: Garmisch-Partenkirchen, Germany; Hampton, Virginia; Mauna Loa, Hawaii; São José dos Campos, Brazil, and SAGE II measurements) were investigated for trend by (1) comparing measurements in the 3 volcanically quiescent periods since 1970 using standard analysis of variance techniques, and (2) analyzing residuals from a time/volcano dependent empirical model applied to entire data sets. A standard squared-error residual minimization technique was used to estimate optimum parameters for each measurement set, allowing for first order autocorrelation, which increases standard errors of trends but does not change magnitude. Analysis of variance over the 3 volcanically quiescent periods is controlled by the end points (pre-El Chichón and post-Pinatubo), and indicates either no change (Garmisch, Hampton, São José dos Campos, Laramie-0.15 μm) or a slight, statistically insignificant, decrease (Mauna Loa, Laramie-0.25 μm), $-1 \pm 0.5\%$ yr^{-1}. The empirical model was applied to the same records plus 1020 nm SAGE II data separated into 33 latitude/altitude bins. No trend in stratospheric aerosol was apparent for 31 of 33 SAGE II data sets, 3 of 4 lidar records, and in situ measurements at 0.15 μm. For Hampton and Laramie-0.25 μm, the results suggest a weak negative trend, $-2 \pm 0.5\%$ yr^{-1}, while 2 SAGE II data sets (30–35 km, 30° and 40°N) suggest a positive trend of similar magnitude. Overall we conclude that no long-term change in background stratospheric aerosol has occurred over the period 1970–2004.

Citation: Deshler, T., R. Anderson-Sprecher, H. Jäger, J. Barnes, D. J. Hofmann, B. Clemesha, D. Simonich, M. Osborn, R. G. Grainger, and S. Godin-Beekmann (2006), Trends in the nonvolcanic component of stratospheric aerosol over the period 1971–2004, *J. Geophys. Res.*, *111*, D01201, doi:10.1029/2005JD006089.

1. Introduction

[2] Observations characterizing the altitudes, sizes, and number concentrations of stratospheric aerosol were first provided by balloonborne impactor measurements in the late 1950s [*Junge et al.*, 1961]. Subsequent measurements by both aircraft- and balloon-borne impactors suggested the global distribution of stratospheric aerosol [*Junge and Manson*, 1961; *Chagnon and Junge*, 1961]. These observations indicated that particles >0.1 μm had a maximum in concentration near 20 km, suggesting an aerosol source in this region [*Junge et al.*, 1961]. These particles were large enough to contribute to the purple twilight noted by early observers [*Gruner and Kleinert*, 1927]. Recent calculations suggest that tropospheric aerosol must also contribute to the purple twilight in cases of a clean stratosphere [*Lee and Hernandez-Andres*, 2003].

[3] *Junge et al.*'s [1961] measurements were at the end of an extended volcanic-free period [*Stothers*, 1996], but did not establish a baseline for stratospheric aerosol. Quantifying the global stratospheric aerosol burden, and describing the role of volcanic eruptions, required long-term measurements which began in the early 1970s using balloonborne particle counters [*Hofmann et al.*, 1975; *Hofmann and Rosen*, 1980; *Hofmann*, 1990]; lidar [*DeFoor et al.*, 1992; *Osborn et al.*, 1995; *Jäger*, 2005]; and in the late 1970s satellite instruments: SAM (Stratospheric Aerosol Measurements) II (1979–1991) [*Pepin et al.*, 1977; *Poole and Pitts*,

[1]Department of Atmospheric Science, University of Wyoming, Laramie, Wyoming, USA.
[2]Department of Statistics, University of Wyoming, Laramie, Wyoming, USA.
[3]Institut für Meteorologie und Klimaforschung, Atmosphärische Umweltforschung (IMK-IFU), Forschungszentrum Karlsruhe GmbH, Garmisch-Partenkirchen, Germany.
[4]National Oceanic and Atmospheric Administration, Boulder, Colorado, USA.
[5]Instituto Nacional de Pesquisas Espaciais, S. J. dos Campos, Brazil.
[6]NASA Langley Research Center, Hampton, Virginia, USA.
[7]Atmospheric, Oceanic, and Planetary Physics, Oxford University, Oxford, UK.
[8]Service d'Aéronomie, CNRS, Institut Pierre Simon Laplace, Jussieu, France.

Table 1. Names, Locations, Dates, Volcanic Explosivity Index (VEI) and SO_2 and Aerosol Loading, When Available, for All Stratospherically Important Eruptions 1960–2003[a]

Name	Latitude	Longitude	Date	Year	VEI	SO_2, Mt	Aerosol, Tg
Aerosol Loading (span)							
Aerosol	8.3 S	115.. E	Mar 17	1963	5		16–30
Agung	8.3 S	115.. E	Mar 17	1963	5		16–30
			May 16		4		
Shiveluch	56.6 N	161.4 E	Nov 12	1964	4+		
Taal	14.0 N	121.0 E	Sep 28	1965	4		
Kelut	7.9 S	112.3 E	Apr 26	1966	4		
Awu	3.7 N	125.. E	Aug 12	1966	4		
Fernandino	0.4 S	91.5 W	Jun 11	1968	4		
Tiatia	44.3 N	146.3 E	Jul 14	1973	4		
Fuego	14.5 N	90.9 W	Oct 14–17	1974	4		3–6
Tobalchik	58 N	160.3 E	Jul 6	1975	4+		
Augustine	59.4 N	153.4 W	Jan 22	1976	4		
Soufriere	13.3 N	61.2 W	Apr 14, 17	1979	3	0.003	
Sierra Negra	0.8 S	91.2 W	Nov 13	1979	3	4.5	
Saint Helens	46.2 N	122.2 W	May 18	1980	5	0.8	
Ulawun	5.0 S	151.3 E	Oct 6 and 7	1980	3	0.2	
Alaid	50.9 N	156 E	Apr 27–30	1981	4	1.1	
Pagan	18.1 N	148 E	May 15	1981	4	0.32	
Nyamuragira	1.4 S	29.2 E	Dec 25	1981	3		
El Chichón	17.0 N	93.2 W	Mar 28	1982	4	8.1	12
			Apr 4		5		
Galunggung	7.3 S	108.0 E	May 17	1982	4		
Colo	0.17 S	121.6 E	Jul 23	1983	4	0.2	
Nevado del Ruiz	4.90 N	73 W	Nov 13	1985	3	0.66	
Augustine	59.4 N	153.4 W	Mar 27	1986	4?	<0.05	
Nyamuragira	1.4 S	29.2 E	Jul 16	1986	4	0.8	
Chikurachki	50.3 N	155.. E	Nov 20	1986	4?		
Kelut	7.9 S	112.3 E	Feb 10	1990	4	0.15	
Pinatubo	15.0 N	120.3 E	Jun 12	1991	6(5+)	17–20	30
Cerro Hudson	45.9 S	73.0 W	Dec 8	1991	5+	3.3	3
Spurr	61.3 N	152.3 W	Jun 27	1992	4	0.2	
Lascar	23.4 S	67.7 W	Apr 19	1993	4	0.4	
Rabaul	4.3 S	152.2 E	Sep 19	1994	4?	0.2	
Kliuchevskoi	56.1 N	160.6 E	Oct 1	1994	4 (3?)	0.1	
Shishaldin	54.8 N	164.0 W	Apr 19	1999	3		
Ulawun	5.05 S	151.3 E	Sep 29	2000	4	<0.05	
Shiveluch	56.6 N	161.4 E	May 22	2001	4?	0	

[a]From *Carn et al.* [2003], *Newhall and Self* [1982], and *Simkin and Siebert* [1994] (also the web pages of the Smithsonian Global Volcanism Network).

1994], SAGE (1979–1981) (Stratospheric Aerosol and Gas Experiment) and SAGE II (1984-present) [*McCormick et al.*, 1979; *Chu et al.*, 1989; *Thomason et al.*, 1997b]. The impact of sulfur rich volcanic eruptions then became obvious and these have been the dominant source of stratospheric aerosol for the past 30 years. Within the last century the most recent 30-year period has been volcanically active. *Sato et al.* [1993] and *Stothers* [1996], using solar and stellar extinction data, show that the previous 120 years were dominated by eight major eruptions. Four of these occurred between 1880 and 1910 and four since 1960. The long-term measurements which began in the 1970s, have captured the complete cycle for three major eruptions with a global stratospheric impact: Fuego (14°N, October 1974, 3–6 Tg of aerosol), El Chichón (17°N, April 1982, 12 Tg) and Pinatubo (15°N, June 1991, 30 Tg) [*McCormick et al.*, 1995]. Within this record there have been four periods when volcanic influences were at a minimum, 1974, 1978–1980, 1988–1991, and 1997 - present. Table 1 summarizes the volcanic activity between 1960 and 2003, including eruptions with volcanic explosivity index (VEI) ≥ 4, and eruptions with a known stratospheric impact. Also in Table 1 the SO_2 and aerosol loading, if available, are included. Most SO_2 estimates are from Total Ozone Mapping Spectrometer

(TOMS) data [*Carn et al.*, 2003]. Missing estimates primarily occur prior to TOMS measurements. Missing estimates since 1979 indicate that information for that volcano was not available.

[4] The VEI, developed by *Newhall and Self* [1982] to characterize volcanoes, is indicative of the volume of ejecta and the height of the eruption column. The height ranges for a VEI of 3, 4, and 5 are 3–15 km, 10–25 km, and >25 km. VEI alone, however, cannot predict stratospheric impact. Only sulfur rich volcanic eruptions provide the sulfur necessary to form sulfuric acid which then condenses with water into tiny droplets which have stratospheric lifetimes of years. Thus VEI must be coupled with the amount of sulfur ejected from the volcano. For example, Mt. St. Helens, with a VEI of 5.0, contained little sulfur (<1 Mt), thus the stratosphere was not greatly perturbed by Mt. St. Helens [*Robock*, 1981], and, if not for El Chichón, stratospheric aerosol would have returned to background within a few years of the eruption. *Schnetzler et al.* [1997] and *Halmer et al.* [2002] have coupled VEI with sulfur emissions to produce a volcanic SO_2 index which is more indicative of the stratospheric impact of a volcano.

[5] Stratospheric aerosol are important for a number of processes which affect the chemical and radiation balance of

the atmosphere [*McCormick et al.*, 1995; *Solomon*, 1999]. During periods of high volcanic aerosol load there is evidence for heterogeneous chemistry on the sulfate aerosol reducing ozone [*Angell et al.*, 1985; *Hofmann and Solomon*, 1989; *Jäger and Wege*, 1990; *Gleason et al.*, 1993; *Deshler et al.*, 1996], for stratospheric warming [*Labitzke and McCormick*, 1992; *Angell*, 1993; *Russell et al.*, 1993], and for tropospheric cooling [*Manabe and Wetherald*, 1967; *Pollack et al.*, 1976; *Dutton and Christy*, 1992; *Hansen et al.*, 1992]. During volcanically quiescent periods, when stratospheric aerosol is in a "background" state unperturbed by volcanism, radiative effects of stratospheric aerosol are negligible but these aerosol still play a role in the budget of several trace gases, in particular NO_x. NO_2 columns were reduced after both El Chichón and Pinatubo [*Johnston and McKenzie*, 1989; *Johnston et al.*, 1992] from the hydrolysis of N_2O_5 on water bearing volcanic sulfuric acid aerosol [*Rowland et al.*, 1986; *Tolbert et al.*, 1988; *Mozurkiewicz and Calvert*, 1988]. At low aerosol loading NO_x increases and induces ozone loss from the nitrogen catalytic cycle [*Crutzen*, 1970]. *Fahey et al.* [1993] provided direct measurements of the anticorrelation of aerosol surface area and the NO_x/NO_y ratio. The hydrolysis of N_2O_5 saturates as aerosol surface area increases above $5-10 \ \mu m^2 \ cm^{-3}$, thus the role aerosol play in controlling NO_x is primarily important during periods of low aerosol loading [*Prather*, 1992]. Changes in NO_x also affects the abundance of ClO_x and HO_x, both of which also react with ozone [*Wennberg et al.*, 1994; *Solomon et al.*, 1996]. The importance of aerosol in stratospheric chemistry first became apparent with the suggestion of its role in polar ozone loss [*Solomon et al.*, 1986]. Long-term stratospheric aerosol measurements had their beginnings about fifteen years prior to this realization.

[6]　The primary emphasis of long-term stratospheric aerosol measurements has been on volcanic events. This is partly due to the significant impact large eruptions have on the stratosphere, to the increased signal they provide for instruments, to the dynamic nature of eruptions and their aftermath, to their global distribution, and to the fact that volcanic eruptions have dominated the signal for 20 of the past 30 years [*Barnes and Hofmann*, 2001; *Deshler et al.*, 2003; *Jäger*, 2005]. The focus here, however, is on long-term variations of nonvolcanic stratospheric aerosol, so called background aerosol.

[7]　Background stratospheric aerosol are defined to be that aerosol which remains in the stratosphere after all clearly identified volcanic aerosol have fallen to levels as to be indistinguishable from nonvolcanic aerosol oscillations. It is anticipated that natural and anthropogenic emissions of sulfur, in the form of COS and SO_2, will then be sufficient to maintain these aerosol in quasi-steady state. During background periods measurements are expected to remain within variations expected due to measurement error, measurement frequency, and nonvolcanic geophysical oscillations, such as induced by season or the quasi-biennial oscillation (QBO). Although serious questions may be raised about the extent to which inter-volcanic periods over the past 30 years have reached background, measurements during these periods provide the only information available to compare stratospheric aerosol in background periods. The best that can be provided is an objective analysis of these measurements.

[8]　The importance of possible changes in background stratospheric aerosol levels led to the analysis of each quiescent period as it appeared in the record. The first of these analyses [*Hofmann and Rosen*, 1980, 1981; *Sedlacek et al.*, 1983] compared the pre-Fuego and pre-El Chichón periods. Comparison of pre-El Chichón measurements with initial measurements of *Junge et al.* [1961], which were at the end of an extensive volcanic-free period, suggested a possible increase of about a factor of five in aerosol concentration at 20 km during the intervening 20 years, leading *Hofmann and Rosen* [1980] to suggest an increase of 9% yr^{-1} in aerosol mixing ratio for aerosol > 0.15 μm radius. *Sedlacek et al.* [1983], comparing globally distributed airborne filter samples during 1974 and 1979, pre-Fuego and pre-El Chichón, suggested a 6% yr^{-1} increase in background stratospheric sulfur mass.

[9]　The question of changes in background stratospheric aerosol was revisited prior to the Pinatubo eruption. *Hofmann* [1990] compared measurements of aerosol mixing ratio for 0.15 and 0.25 μm radius thresholds during volcanically unperturbed periods in 1974, 1979, and 1989. No change was observed in the mixing ratio of 0.15 μm particles; however, there was a 50% increase in aerosol mixing ratio for particles > 0.25 μm between 1979 and 1989, leading Hofmann to estimate an increase in aerosol mass on the order of 5% yr^{-1} over the decade, consistent with the earlier estimates of *Hofmann and Rosen* [1980] and *Sedlacek et al.* [1983]. A similar increase over the same time period was observed when SAGE I and II measurements were compared; however, *Thomason et al.* [1997a] suggested that 1989 may not have been at true background, due primarily to Nevado del Ruiz in 1985. Increases in tropospheric COS [*Montzka et al.*, 2004] and SO_2 [*van Aardenne et al.*, 2001] over this period suggest an increase of 1–2% in aerosol mass, about half of the increase concluded by *Hofmann* [1990].

[10]　Resolution of the questions raised by these studies had to wait for the third background period in the modern record, the present post Pinatubo period. Based on long-term lidar measurements at Mauna Loa, Hawaii, *Barnes and Hofmann* [1997] suggest that the decay of aerosol loading following El Chichón and Pinatubo was influenced by the phase of the QBO in tropical stratospheric winds (also evident in the Garmisch lidar data [*Jäger*, 2005]) and that integrated aerosol backscatter in 1995 was below any previous observation at Mauna Loa. *Hayashida and Horikawa* [2001] used SAGE II extinction measurements to derive Ångström parameters and concluded that the pre-Pinatubo period was still influenced by volcanic eruptions from the mid-1980s and cannot be considered a real background period. *Barnes and Hofmann* [2001] used the present background period, extending from 1996, to demonstrate variability correlated with the phase of the QBO, with implications for the source of background stratospheric aerosol. Thirty year records of in situ [*Deshler et al.*, 2003] and remote [*Jäger*, 2005] midlatitude measurements suggest that stratospheric aerosol levels in the post-Pinatubo period are at or below any previous background period since 1970. These analyses of the post-Pinatubo aerosol suggest, in contrast to studies of earlier background periods, no long-term increase in stratospheric background aerosol.
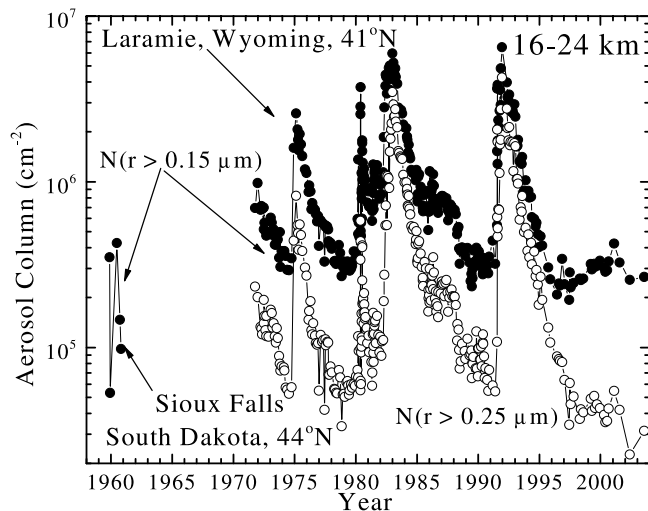
Figure 1. Aerosol columns, 16–24 km, for balloonborne in situ measurements of particles with radius > 0.15 μm (solid circles) above Sioux Falls (43.6°N, 96.7°W), 1959–1960 [*Chagnon and Junge*, 1961], and above Laramie (41.3°N, 105.7°W), 1971–2003 [*Deshler et al.*, 2003]. Also included in the Laramie measurements are particles with radius > 0.25 μm (open circles).

[11] Figure 1 compares the long-term aerosol measurements from Laramie, Wyoming, initiated by *Hofmann et al.* [1975], with Junge's initial measurements at nearly the same latitude [*Chagnon and Junge*, 1961]. Based on instrumental characteristics, *Junge et al.* [1961] suggest that their measurements collected particles >0.15 μm radius with a 55% efficiency. The integrals shown in Figure 1 account for this collection efficiency and use a 100% collection efficiency for the Wyoming measurements, the case which would lead to the minimum difference between measurements. The comparisons with Junge's measurements shown in *Hofmann and Rosen* [1980] assumed the same collection efficiency applied to both sets of measurements. Accounting for this collection efficiency on only one side would have reduced *Hofmann and Rosen*'s [1980] estimate to 6% yr^{-1}, instead of 9% yr^{-1}. Comparing the average of Junge's measurements shown in Figure 1 with the minimum in column integrals observed in 1979 suggests a more conservative increase of 2% yr^{-1}, but, as apparent from Figure 1, would have still suggested a significant increase in background aerosol.

[12] During volcanically quiescent periods the sulfur for stratospheric aerosol arises from the transport of tropospheric COS, SO$_2$, and sulfate aerosol into the stratosphere. The fractional contributions of COS, SO$_2$, and sulfate aerosol to stratospheric aerosol are approximately 35, 25, and 40%, obtained by combining estimates from *Weisenstein et al.* [1997] and *Pitari et al.* [2002]. Between 1960 and 1980 anthropogenic emissions of SO$_2$ increased by over 2% yr^{-1}. Assuming that natural sources of SO$_2$ remained fairly constant at about 30% of total SO$_2$ emissions [*Pitari et al.*, 2002], this implies an increase of ∼1.6% yr^{-1} in SO$_2$ emissions between 1960 and 1980 [*van Aardenne et al.*, 2001]. During this same period COS increased at a rate of approximately 0.5% yr^{-1} [*Montzka et al.*, 2004]. If these increases in SO$_2$ and COS are weighted according to their fractional contribution to stratospheric aerosol, assuming that the contribution of sulfate aerosol remains constant, and that stratospheric aerosol responds linearly with respect to source gases, then the increase in stratospheric aerosol can be estimated. These estimates indicate an increase of ∼0.6% yr^{-1}, well below *Hoffman and Rosen*'s [1980] estimate of 9% yr^{-1} and even the more conservative estimate of 2% yr^{-1} indicated in Figure 1. A linear response to changes in source gases is consistent with sensitivity studies to changes in COS performed with a 2-D model [*Weisenstein et al.*, 1997; *Weisenstein and Bekki*, 2006].

[13] The stability of the post Pinatubo Wyoming aerosol measurements, and the scatter in the initial measurements of *Chagnon and Junge* [1961] leads to questions concerning the initial measurements. Was the sampling efficiency of the instrument fully accounted for, or was the instrument sensitive to particles somewhat larger than 0.15 μm? The latter question was considered earlier, but dismissed [*Hofmann and Rosen*, 1981]. In any case it is clear from Figure 1 why initial measurements in the late 1970 background period was interpreted as indicating an aerosol increase [*Hofmann and Rosen*, 1980, 1981]. The existence of a number of long-term stratospheric aerosol records lets us now revisit the question of the stability of background stratospheric aerosol.

[14] The purpose here is to examine all long-term stratospheric aerosol measurements for trends in the background aerosol. This requires records which span at least two of the four volcanically quiescent periods in the modern aerosol record, limiting the data set to the six longest stratospheric aerosol measurement records available, one in situ record, four lidar records and one satellite record. The satellite record began in 1982, the other records in the 1970s. This work forms part of the *SPARC Assessment of Stratospheric Aerosol Properties* where more detail on the following analyses can be found [*Deshler and Anderson-Sprecher*, 2006].

2. Instruments

2.1. In Situ Measurements

[15] Stratospheric aerosol measurements above Laramie, Wyoming (41.3°N, 105.7°W), began in 1971 using an optical particle counter (OPC) initially developed by *Rosen* [1964]. The instrument measures the intensity of scattered white light at 25° in the forward direction from single particles passing through the light beam. Since the illuminated volume is larger than the aerosol stream, the sampling efficiency is high. Mie theory is used to determine aerosol size from the amount of scattered light. The Light is collected over a solid angle of ∼0.17 steradian and focused onto a photomultiplier tube (PMT) for pulse height detection. Two symmetrical independent photon paths limit noise, Rayleigh scatter, and the influence of cosmic rays by coincidence counting. Single coincident PMT pulses which exceed preset voltage levels are counted and used to determine aerosol concentration and size. Prior to each flight the instruments are calibrated with polystyrene latex spheres and the pump flow rate measured. Periodically the stability of the pumps throughout flight range pressures is checked, and the theoretical counter respose function checked against PSL and monodispersed diethyl hexal

sebacate at several sizes. See *Deshler et al.* [2003] for additional details.

[16] Initial measurements in the 1970s consisted of measurements of the concentration of particles with radius ≥ 0.15 and 0.25 μm at a sample flow rate of 1 liter min^{-1} [*Pinnick and Hofmann*, 1973; *Hofmann et al.*, 1975]. In 1989, the OPC was modified to include measurements of particles >0.4 μm, to increase the number of sizes measured, and to reduce the minimum concentration threshold [*Hofmann and Deshler*, 1991]. The scattering angle of the detector axis was increased from 25 to 40° and the air sample flow rate increased from 1 to 10 liters min^{-1}, with appropriate changes in inlet design to maintain roughly isokinetic sampling. This new scattering angle allowed unambiguous detection of particles throughout the size range 0.15 − 10.0 μm. After 22 calibration flights in Laramie to insure that the measurements at 0.15 and 0.25 μm radius are, within measurement limits, the same for counters with scattering angles at 25 and 40°, the new OPC replaced the old OPC for regular flights in Laramie beginning in 1991 [*Deshler et al.*, 1993, 2003].

[17] A more complete description of the instrument and discussion of error sources is provided in *Deshler et al.* [2003]. Here we summarize the primary error sources. Sizing errors of ± 10% at 0.15 and 0.25 μm result primarily from pulse broadening by photo multiplier tubes. Errors in concentrations are controlled by Poisson counting statistics or a precision of ±10% when Poisson counting statistics are not a factor. Poisson uncertainties lead to concentration uncertainties of 85, 25, and 8% for concentrations of 0.01, 0.1, and 1.0 cm^{-3} at a sample rate of 1.0 liter min^{-1} and concentrations of 0.001, 0.01, 0.1 cm^{-3} at 10 liters min^{-1}.

2.2. Remote Lidar Measurements

[18] The first lidar (light detection and ranging) measurements of stratospheric aerosol were completed shortly after *Junge et al.*'s [1961] initial measurements [*Fiocco and Grams*, 1964]. Lidar sites investigating stratospheric aerosols now range in latitude from 90°S to 80°N, with a number of sites in northern midlatitudes, and a few stations in the sub tropics and southern midlatitudes. Lidars provide remote, vertically resolved measurements of atmospheric backscatter from both molecules and aerosols at one or more wavelengths. To obtain aerosol backscatter profiles from a lidar requires accounting for three factors which affect the backscattered light received by the lidar telescope: (1) two way light extinction, (2) molecular backscatter, and (3) instrument normalization [e.g., *Russell and Hake*, 1977]. Molecular backscatter and extinction is typically calculated from pressure/temperature profiles provided by a nearby radiosonde station.

[19] Uncertainties in lidar measurements arise from two-way extinction of the lidar signal, the difficulty of determining an aerosol free region for normalization, signal induced noise, and from detector nonlinearity for analog detection systems, or pulse overlapping for photon counting systems. For volcanic conditions there is a large aerosol signal, well above the molecular signal, resulting in small uncertainties. For quiescent conditions aerosol backscatter is less than 5% of molecular scattering, requiring longer integration times. The two-way particle extinction of the lidar signal becomes significant during periods of high

aerosol loading but is reduced considerably for measurements during background periods [*Simonich and Clemesha*, 1989]. The purely instrumental errors from effects such as signal-induced noise can be reduced significantly by careful instrumental design. Long-term calibration problems do not arise because, for each measurement, aerosol back-scatter is determined only after the lidar signal is forced to match that expected from a purely molecular atmosphere at the altitude of normalization. The main source of error is in uncertainties in the molecular profile corresponding to a given lidar profile. The sources of molecular profiles and the estimated precision are given below for each of the lidar series used in this study.

[20] The four lidar records included here are the only multi-decadal lidar records available. They are based at São José dos Campos, Brazil (23.2°S, 45.9°W, 1971–2003), Mauna Loa, Hawaii (19.5°N, 156°W, 1974–2004), Hampton, Virginia (37.1°N, 76.3°W, 1974–2002), and Garmisch-Partenkirchen, Germany (47.5°N, 11.1°E, 1976–2002). To reduce variations in the measurements due to variations in altitude and thickness of the aerosol layer, the quantity used for long time series comparisons is the vertically integrated backscatter coefficient with units of sr^{-1}.

[21] The São José dos Campos measurements use the sodium D2 line at 589 nm and began in 1972. Although the primary focus is on the atmospheric sodium layer, measurements of stratospheric aerosol are also available [*Clemesha and Simonich*, 1978; *Simonich and Clemesha*, 1997]. The wavelength used for the measurements has not changed during the period, although there have been major changes in the laser and improvements in the electronics. Since this site is in the sub tropics, tropopause height fluctuations and variations in the atmospheric density profile are minor. The molecular density profile used is an annual average derived from rawinsonde measurements. An iterative procedure is used to account for aerosol extinction. Ozone absorption is negligible. The measurements presented here represent monthly averages of integrated aerosol backscatter from 17 to 35 km. Error estimates on the integrated profiles are ±5%.

[22] The Mauna Loa, Hawaii, measurements, using a ruby laser, 694 nm, began in 1974 [*DeFoor et al.*, 1992; *Barnes and Hofmann*, 1997, 2001]. In 1994 a new lidar was installed using a Nd:YAG laser measuring backscatter at both the 532-nm harmonic and the 1064-nm fundamental. For data continuity, the 532-nm measurements are converted to 694 nm for easy comparison with the early measurements. Errors on the integrated backscatter range from ±15 to > ±30% for the ruby measurements, depending on aerosol load. These errors reduce to approximately ±6% for the 532-nm measurements. Tropopause fluctuations are minor and the altitude interval for backscatter calculation is fixed at 18 to 33 km. Molecular density is obtained from a model for the Ruby lidar analysis and from the nearest radiosonde site (Hilo, Hawaii) for the Nd:YAG lidar. There was an overlapping period of about a year (40 observations) during which backscatter at both wavelengths was measured. The average absolute backscatter of the ruby lidar agreed to within 2% of the Nd:YAG backscatter interpolated to 694 nm from the measurements at 532 and 1064 nm.

[23] The Hampton, Virginia, measurements also use a ruby laser and began in 1974 [*Fuller et al.*, 1988; *Woods et*

al., 1994; *Osborn et al.*, 1995]. Although there have been incremental improvements in the system, the fundamental operating wavelength and measurement principles have not changed. For this midlatitude station the integration interval is from the tropopause to 30 km. Errors range from 15–50% during stratospheric background periods reducing to 5% for measurements following large eruptions. Molecular densities are obtained from a radiosonde station 120 km to the northeast.

[24] The Garmisch-Partenkirchen, Germany, measurements began in 1976 with a ruby laser [*Reiter et al.*, 1979; *Jäger*, 2005]. There was an interruption in the measurements from May 1990 to March 1991 to convert the lidar to a Nd:YAG system. Measurements beginning in 1991 use the 532-nm harmonic of the Nd:YAG laser. As in the case of Mauna Loa, all 532-nm measurements are converted to 694 nm to easily compare with the earlier measurements. Backscatter integrations cover the altitude range, tropopause +1 km to profile top. Error estimates range from 10 to 50%, depending on stratospheric aerosol load, for the ruby measurements. These errors are reduced by about half for the 532-nm measurements. Molecular density is obtained from a radiosonde station at Munich, 100 km to the north. Iteration is used to account for aerosol extinction.

2.3. Remote Satellite Measurements

[25] The first regular measurements of stratospheric aerosol by satellite were completed by SAM II [*McCormick et al.*, 1979, 1981; *Russell et al.*, 1981]. The multiwavelength SAGE and SAGE II instruments [*Mauldin et al.*, 1985] followed close behind. These instruments are self calibrating since prior to or after each solar occultation the photometer measures the direct solar transmission without atmospheric extinction. Of the eleven instruments deployed on satellites in the past 30 years which include stratospheric aerosol measurements, only SAGE II has a record long enough to consider for our purposes. This record can be extended somewhat by SAGE I. SAM II measurements span 12 years, 1979–1991, at high latitudes, 72–83° N/S [*Poole and Pitts*, 1994]. Although SAM II measurements are not strongly affected by volcanic eruptions, they have a strong annual cycle and wintertime measurements are influenced by polar stratospheric clouds. This coupled with the relatively short record limited our interest in SAM II to a simple inspection of the measurements, which does not show any clear temporal tendency. Only the SAGE II record was considered of sufficient length to be evaluated for trends.

[26] SAGE II measures solar transmission through the atmosphere with a spectral radiometer. To convert this to aerosol extinction the influence of gas molecules along the tangent line of sight must be removed, as well as gas and aerosol extinction from altitudes above the measurement altitude. The extinction at upper altitudes influences a measurement at the leading and tailing boundaries along the line of sight due to the spherical geometry. Removing these contributions is known as the onion peeling method. The inversion of the SAGE II solar occultation measurements to provide aerosol extinction is described by [*Chu et al.*, 1989]. The effect of subtle changes in the SAGE II instrument are carefully monitored and are routinely eval-

uated for impact on data products including ozone and aerosol extinction [*Thomason and Burton*, 2006]. The 1020-nm aerosol extinction exhibits extremely limited sensitivity to changes in instrument characteristics like unobscured solar intensity measurements, dark current, and mirror reflectivity. The 525-nm aerosol channel is slightly more sensitive to such changes, but even there, the possible drift over the lifetime of the instrument is <1%. Since SAGE II uses National Center for Environmental Protection (NCEP) estimates of molecular density for the computation of the molecular contribution to the line-of-sight transmission, a long-term drift between NCEP temperatures and the real atmosphere could introduce a drift of a few percent over the lifetime of the instrument. There has been a number of validation efforts [*Russell et al.*, 1984; *Osborn et al.*, 1989; *Oberbeck et al.*, 1989; *Russell and McCormick*, 1989; *Hervig and Deshler*, 2002]. As the understanding of the instrument performance has evolved a number of revisions of the SAGE II data have been provided; however, for our purposes the revisions are not critical. For any one revision the same data inversion is applied to all past measurements, thus the relative values of extinction over a 20 year period will stay the same even though the absolute values may change from one revision to another.

3. Measurements

[27] For the quantitative comparison of volcanically quiescent periods, the primary measurement from each instrument will be used. The measurements have been checked to be cloud and tropospheric aerosol free and are at latitudes ≤50°. They thus will not be perturbed by polar stratospheric clouds.

[28] For the in situ measurements approximately monthly profiles of aerosol concentration for particles ≥0.15, 0.25 μm are integrated over altitude columns varying from 5 to 15 km. Typical tropopause heights at Laramie are 10–12 km extending to 15 km in the summer. Column integrals from 15–20 and 20–25 km are presented in Figure 2. For reference global anthropogenic SO_2 emissions since 1970 are shown in Figure 2b. The 1970–1990 estimates are from *van Aardenne et al.* [2001]. The 2000 SO_2 emissions are estimated based on extrapolating the 1990 estimate with a -2% yr^{-1} trend [*Hicks et al.*, 2002].

[29] In Figure 2, the 0.15 μm column integrals plateau at similar values at both altitude intervals for the three background periods, while the 0.25 μm measurements show a bit more variation, remaining elevated in 1990–1991 compared to 1979 and 1997, particularly between 15 and 20 km. The 0.25 μm observations prior to Pinatubo were the reason for *Hofmann*'s [1990] estimate of a 5% yr^{-1} increase in sulfur mass between 1979 and 1989.

[30] The final measurements in 2002 and 2003 show striking variations, but suffer from a sampling frequency reduced to once per year. The particularly low measurement in 2002, 20–25 km, was checked carefully and was confirmed by two independent simultaneous measurements at 0.25 μm. Thirty day isentropic back trajectories at 570 and 690 K (~24 and 27 km) do not provide any useful insight into why the concentrations are low. The SAGE II data during this period do not show any corroborating areas
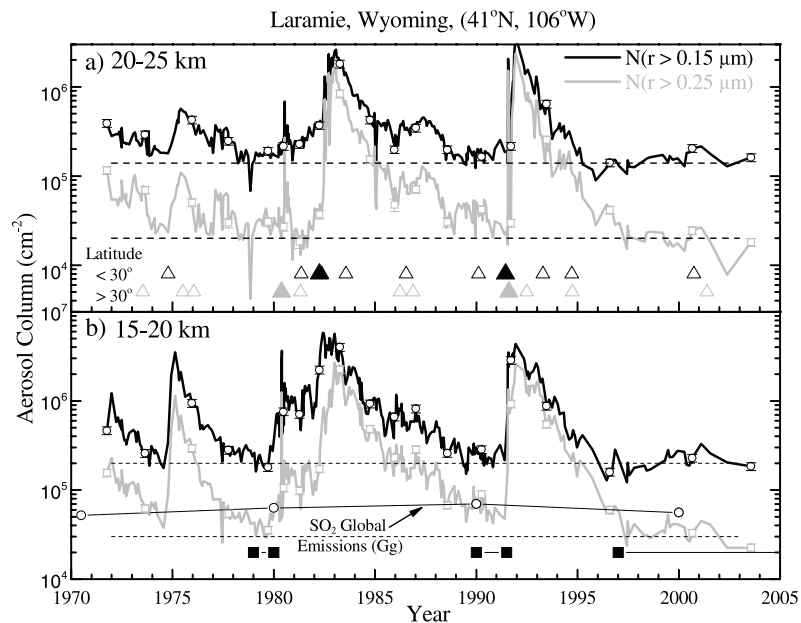
Figure 2. History of column integrals of aerosol number for particles with radii >0.15 and >0.25 μm from in situ measurements above Laramie, Wyoming, United States, (a) 20–25 km, (b) 15–20 km. The measurements represent about 340 individual aerosol profiles. The error bars on the occasional measurement represent the counting error of the measurement and rarely exceed the size of the data symbol. The dashed lines are horizontal and are meant only to aid the reader. The times of the most significant volcanic eruptions during the period are indicated with triangles in Figure 2a, separated into those eruptions at latitudes less (upper symbol) and greater (lower symbol) than 30°. Eruptions with VEI of 5 (large solid symbol) and 4 (small open symbol) are shown. Names of the eruptions are listed in Table 1. Global emissions of SO_2 (Gg of S) are shown in Figure 2b for 1970–1990 [*van Aardenne et al.*, 2001]. The scale for aerosol column also applies for Gg of sulfur. The 2000 estimate is based on a 20% decrease since 1990 [*Hicks et al.*, 2002]. The regions bounded by boxes in the bottom of Figure 2b represent investigator determined background periods.

of clean air, nor are there any significant changes in the variance of the SAGE II extinction measurements. Thus there are no simple explanations for this observation of surprisingly low concentrations at 0.25 μm between 20 and 25 km.

[31] Histories for integrated backscatter from the low and midlatitude lidars are shown in Figure 3. The extremely low São José measurements prior to 1975 have been compared to northern hemisphere measurements in the same time period [*Clemesha and Simonich*, 1978]. The São José 20 km aerosol backscatter, β_a, was about half that measured in the northern hemisphere in 1973 using an airborne lidar operating at nearly the same wavelength [*Fernald and Schuster*, 1977]. Only the Hampton, Virginia, lidar measurements extend into 1974, and these are in general quantitative agreement with the upper range of the early São José measurements. The suggestion from the São José measurements, of the lowest aerosol loading in the record prior to 1975, is not corroborated by similarly low in situ measurements in the northern hemisphere, Figure 2. *Clemesha and Simonich* [1978] suggest the Fuego aerosol did not appear in the southern hemisphere until April 1975 due to the inhibition of eddy transport in 1974 by the meridional circulation in northern winter. There is an aerosol increase in late 1973, following the early 1973 Fuego eruption, and again in early 1975, following the late 1974 Fuego eruption, which appears to be the largest of the three eruptions.

[32] The São José measurements in the early 1980s, prior to El Chichón, are in agreement with the Mauna Loa measurements. São José measurements are slightly elevated in the background period prior to Pinatubo compared to Mauna Loa measurements and to São José measurements in the period following Pinatubo. The similarity of the fluctuations between São José and Mauna Loa in the 1998–2002 period is striking. From the Mauna Loa lidar, the pre- and post-Pinatubo periods are similar, although the variation of the signal in the pre-Pinatubo period is much less than post Pinatubo variability. For the São José measurements the pre- and post-Pinatubo periods are both characterized by significant fluctuations.

[33] The midlatitude lidars are in quite good agreement throughout the record. The peak integrated backscatter following Pinatubo and El Chichón are similar as are the decay rates. The relaxation of the stratosphere following El Chichón is delayed by several minor eruptions. This feature is also apparent in the in situ measurements particularly in the 15–20 km column. Considering the background periods, both lidars agree suggesting that the pre-El Chichón and post-Pinatubo periods are similar, whereas the pre-Pinatubo period is elevated. This again is similar to the in situ measurements for 0.25 μm particles between 15 and 20 km. This correspondence between in situ 0.25 μm measurements and integrated lidar backscatter has been noted before [*Jäger and Hofmann*, 1991; *Hofmann et al.*, 2003].
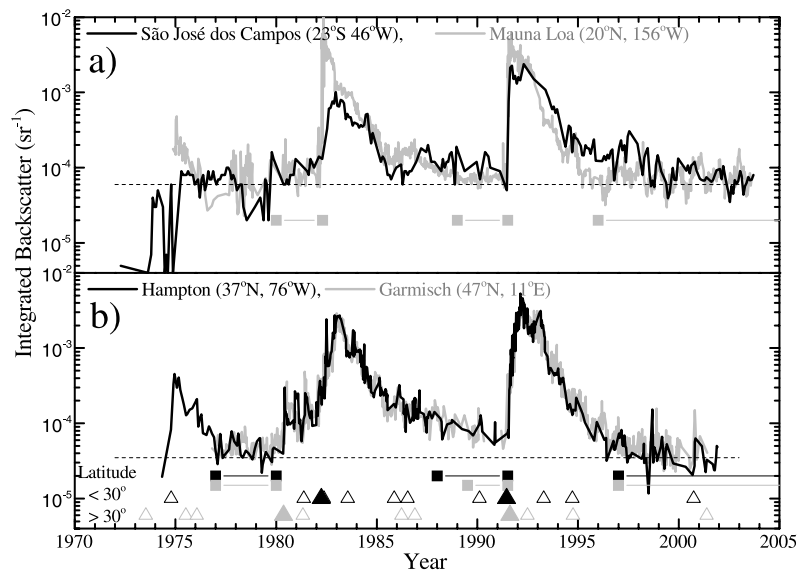
Figure 3. History of integrated backscatter from two tropical sites (São José dos Campos and Mauna Loa) and two midlatitude sites (Hampton and Garmisch). The wavelengths for all measurements are 694 nm except for São José which is at 589 nm. (a) São José dos Campos, Brazil, integration from 17–35 km, and Mauna Loa, Hawaii, United States, integration from 15.8–33 km. (b) Hampton, Virginia, United States, integration from tropopause to 30 km, and Garmisch-Partenkirchen, Germany, integration from tropopause+1 km to layer top. Error estimates range from 5 to 50% and are somewhat dependent on the aerosol load. The dashed lines are horizontal and are meant only to aid the reader. The times of the most significant volcanic eruptions during the period are indicated in Figure 3b with triangles, separated into those eruptions at latitudes less (upper symbol) and greater (lower symbol) than 30°. Eruptions with VEI of 5 (large solid symbol) and 4 (small open symbol) are shown. Names of the eruptions are listed in Table 1. The regions bounded by squares in the bottom of both panels represent investigator determined background periods for Mauna Loa, Hampton, and Garmisch.

4. Investigation of Trends in the Long-Term Aerosol Measurement Records

[35] Previous analyses of long-term trends in background stratospheric aerosol have been limited to comparisons of the aerosol record during volcanically quiescent periods and with *Junge et al.*'s [1961] initial measurements [*Hofmann* *and Rosen*, 1980, 1981; *Sedlacek et al.*, 1983] The increase that these investigators reported can be seen in Figure 1. Figure 1 also indicates that in the midlatitudes in the 1970s the periods when stratospheric aerosol may have reached background were short, ~1–2 years.

[36] The 1970s were dominated by one large tropical eruption, Fuego, and no small tropical eruptions, Table 1 and Figures 2 and 3. All other eruptions were at high latitudes. In contrast the 1980s were dominated by one large tropical, El Chichón, and several smaller tropical eruptions. The smaller tropical eruptions, particularly Nevado del Ruiz, interrupted the decay from El Chichón and led to some controversy about whether stratospheric aerosol had reached background prior to Pinatubo [*Hofmann*, 1990; *Thomason et al.*, 1997a]. This discussion highlights one of the problems inherent in a comparison of background periods. Has background been reached? In hindsight it now seems clear, based on the volcanically quiescent period following Pinatubo, that background was not reached prior to Pinatubo [*Barnes and Hofmann*, 2001; *Hayashida and Horikawa*, 2001], Figures 2, 3, and 4.

[37] The statistical analysis here will follow two approaches. The first will follow the lead of previous investigators and compare the 3 volcanically quiescent periods in the 5 long-term data sets which capture these. The second will use an empirical model to remove the volcanic signal from the long-term records and investigate the residuals for trends. This approach permits the SAGE
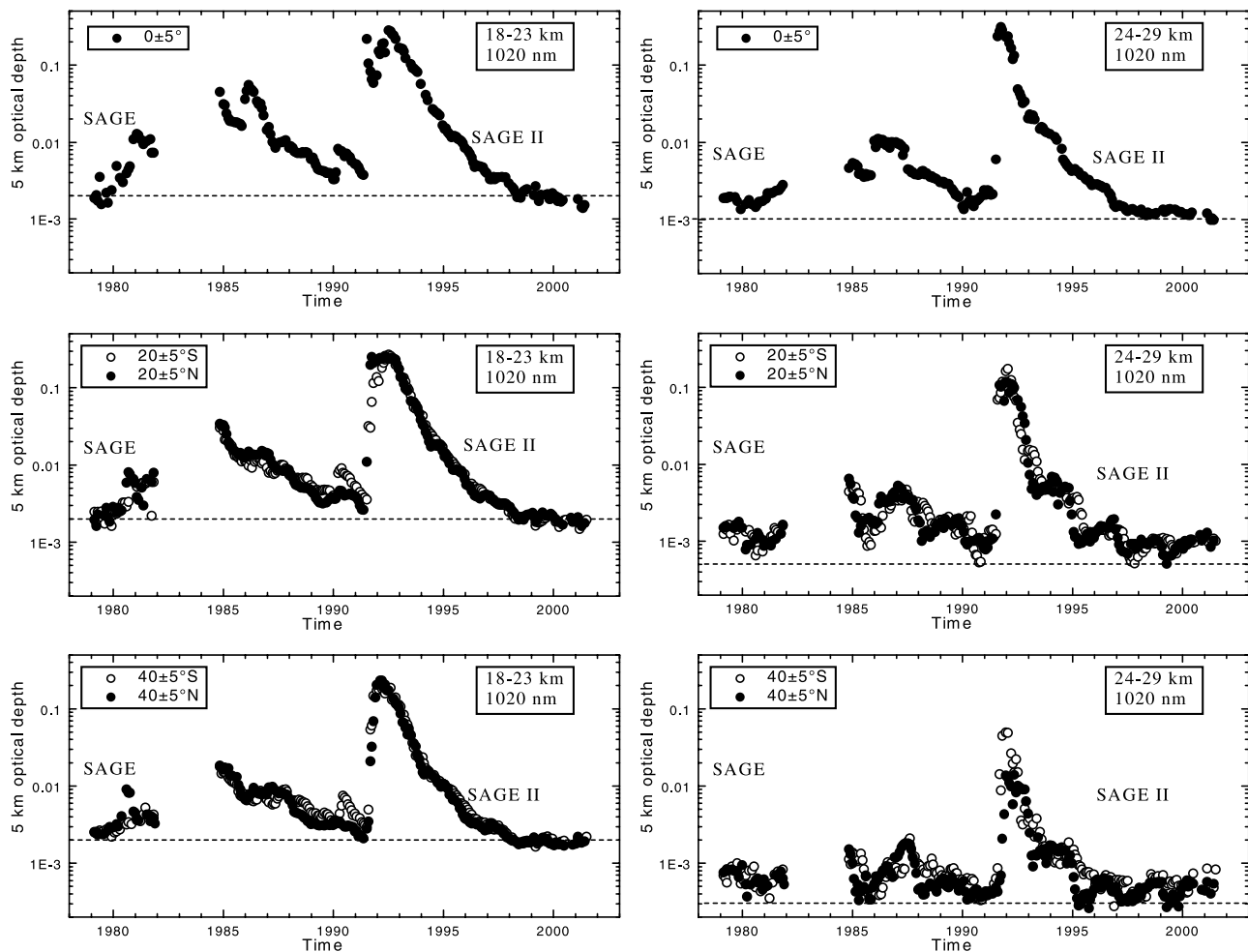
Optical depths for zonally averaged SAGE and SAGE II aerosol extinctions at 1020 nm over the period 1984–2001 are shown in Figure 4. The data are zonal averages binned in 10° latitude intervals at the Equator, ±20° and ±40°. The base altitude, 18 km, was chosen to remove any influence of tropospheric aerosol or clouds. These figures show the decaying volcanic signal of El Chichón followed by the strong increase then decay in optical depth following the eruption of Mt. Pinatubo. The optical depth decreases with increasing latitude. This is mostly caused by calculating the optical depth for a constant altitude range. As the tropopause height lowers towards the poles the aerosol layer also descends, effectively lowering the optical depth for a fixed altitude range. The difference between the Northern and Southern Hemispheres is within the random uncertainty which is typically ±20%. The major exception to this is during the Pinatubo peak, 24–29 km, when aerosol was still forming and the difference is most likely explained by stronger transport into the winter hemisphere from the tropics.

[34] note: The paragraph beginning "Optical depths" is paragraph [34].

Figure 4. Zonal averages, ± 5°, of SAGE and SAGE II 1020 nm optical depths versus time centered at 0, ±20 and ±40°. Left column optical depth integrated from 18 to 23 km. Right column optical depth from 24−29 km. Open (solid) symbols are for the Southern (Northern) hemisphere.

data to be included. These analyses do not account for the impact of trends in stratospheric water vapor and temperature on aerosol size, but this appears to be minor.

[38] Given sulfuric acid mass, water vapor pressure, and temperature, the composition of stratospheric aerosol can be predicted from thermodynamics [*Steele and Hamill*, 1981]. Using aerosol composition and assuming a lognormal size distribution with constant width, the median radius of the aerosol can also be predicted. Over the record of long-term stratospheric aerosol measurements there have been increases in stratospheric water vapor of at most 10% decade^{-1} [*Oltmans and Hofmann*, 1995; *Kley et al.*, 2000], and decreases in stratospheric temperature of 0.5 K decade^{-1} [*Ramaswamy et al.*, 2001]. Since both of these changes would lead to larger particles, the effects of these maximum possible changes were estimated to see if they were significant. The changes in water vapor and temperature were used to estimate the fractional change in particle median radius and composition. The changes were found to be less than 10^{-4} μm decade^{-1} in size and −0.5% decade^{-1} in sulfuric acid weight fraction in the lower to middle stratosphere between 70°S and 70°N. These changes of aerosol in volcanically quiescent periods are not observable

in the measurements available for comparison. In addition, *Nedoluha et al.* [2004] suggest the trend in water vapor may not be as high as 10% decade^{-1} leading to even less of a change in aerosol size.

4.1. Comparison of Stratospheric Aerosol During Nonvolcanic Periods

[39] The results of a comparison of measurements in background periods will depend in large measure on how the periods are specified. While defining background periods is relatively straight forward, specifying background periods is fraught with difficulty since (1) most stratospheric volcanic aerosol decay processes display an exponential rather than linear character, (2) there can be input from minor eruptions between major eruptions, such as after El Chichón, (3) recent history has been relatively volcanically active, and (4) the time periods for some background periods can be exceedingly short. At least 70% of the period between 1971 and 1997 was perturbed by volcanic activity. In spite of these difficulties the in situ, 15−30 km column, and lidar, integrated backscatter, measurements are used to compare the measurements during the three background periods identified for each data set. This analysis is com-
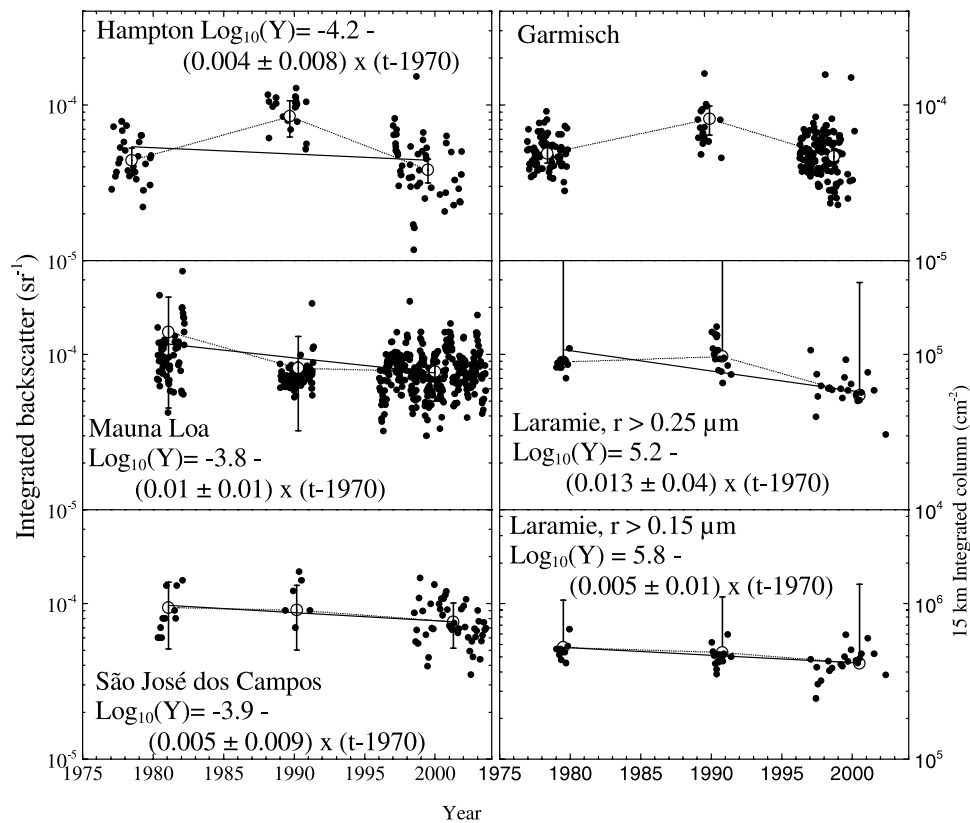
Figure 5. Comparison of measurements during three investigator determined background periods for integrated backscatter measured above Garmisch, Hampton, Mauna Loa, and São José dos Campos, and for column integrals, 15–30 km, of aerosol concentration for particles ≥ 0.15, 0.25 μm above Laramie. Means and 95% confidence intervals (∼±2 standard errors) for each background period are shown (symbols with error bars connected with a dashed line) along with a linear regression (solid line) when convergence, including autocorrelation, was achieved. This is the case for all but Garmisch. The confidence intervals account for autocorrelation and may be overly large for Laramie because of strong autocorrelations in the presence of sparse data. The interval on the ordinate for each graph is the same so that even though magnitudes of the aerosol measure differ between the lidar and in situ measurements, the slopes are comparable.

pleted because it is straight forward and has been the approach of all preceding analyses of background stratospheric aerosol. The background periods were identified by each investigator based on their individual criteria, Figures 2 and 3. While a more objective approach would be preferable, the variation in the measurements and the sometimes brief background periods are not amenable to a more objective analysis. The approach followed allows experimentalists, using their understanding of the measurement technique, and characteristics of stratospheric aerosol, to manually inspect the record and select time periods free of volcanic aerosols. Although this method is the most subjective, it benefits from the investigator's experience in recognizing the effects of volcanic activity. The method relies on a subjective assessment of when the characteristic decay of aerosol mixing ratio or integrated backscatter, following a volcanic eruption, no longer influences the record. The background periods identified by the experimentalists at Hampton and Garmisch are equivalent except prior to Pinatubo (Figure 3b), adding some credibility to investigator determined background periods. The back-

ground periods for Mauna Loa were used also for the São José dos Campos data, except after Pinatubo, then the São José dos Campos background period was begun in 1998.5. The sensitivity of this analysis to the choice of background periods was tested by changing the background periods selected by ± 0.5 yr. These changes did not significantly affect the following results.

[40] The comparisons of background periods were completed using analysis of variance with adjustment for autocorrelation to compare the data within each of the three background periods for each data set, and by applying a linear regression model to the log of the aerosol measure versus time to investigate temporal changes in the background periods. Figure 5 presents for each data set, the background data, means and 95% confidence intervals for sample means during each background period, and the results from a linear regression model applied to the data. The 95% confidence intervals account for autocorrelation.

[41] The analysis of variance tests indicate little difference between the means of the first and third background periods. A statistically significant increase was observed for

the middle period, pre-Pinatubo, for the Laramie-0.25 μm, Garmisch, and Hampton data. This increase in the background prior to Pinatubo has been discussed by *Hofmann* [1990] and *Thomason et al.* [1997a] and is clearly evident in the high northern latitude sites in Figure 5, except for the Laramie-0.15 μm data. It now seems clear that this period was still perturbed by residual volcanic activity, either from Kelut in 1990 or remnants from Nevado del Ruiz in 1985. The other site to show a difference is Mauna Loa where the data suggest that the first background period is elevated compared to the pre- and post-Pinatubo periods, which show no significant difference.

[42] The linear regression for the three background periods analyzed suggests a weak negative trend, $-0.5 \pm 0.5\%$ yr^{-1} for the Laramie 0.15 μm, Hampton, and São José dos Campos measurements and $-1 \pm 0.5\%$ yr^{-1} for Laramie 0.25 μm and Mauna Loa measurements. Convergence criteria for linear regression were not met for Garmisch. If autocorrelation is ignored these results suggest a negative trend in stratospheric aerosol for the Laramie 0.25 μm and Mauna Loa measurements, which is significant. The data, however, are not independent. Autocorrelations at the scale of one month were estimated between 0.70 and 0.98, values which strongly affect inference. Unequal time spacing and the autocorrelations were accommodated by appealing to a one-dimensional spatial model, equivalent to a first-order autoregressive error regression model [*Cressie*, 1993]. The results are compelling in that data which suggest changes in background without accounting for autocorrelations (Laramie-0.25 μm, Mauna Loa, Figure 5) do not suggest any trend when autocorrelation is accounted for. Although estimates of growth/decay rates change little, standard errors typically about triple when the more appropriate model is used, leading to the large error bars shown.

[43] This analysis follows the lead of the early comparisons of background periods, but concludes that there is no long-term trend in background aerosol. This is in agreement with other recent comparisons of background periods using single data sets [*Barnes and Hofmann*, 1997, 2001; *Deshler et al.*, 2003; *Jäger*, 2005].

4.2. Removing the Volcanic Signal From the Long-Term Measurement Records

[44] The second approach to analyze for trends in background aerosol seeks to remove the major perturbing signal, the volcanic effects, from the data and analyze the resulting baseline for trend. Techniques applicable to a wide range of observations and which do not require a priori knowledge of the unique behavior of a particular data record are used. The advantage of this approach is to transform the ~30 year measurement records from ones limited to comparisons of 2–3 time periods, which range from 1 to 5 years, to a record which includes the entire set of measurements. Considering that the longest satellite record, SAGE II, captures just two nonvolcanic periods this is the only approach that can take advantage of this global 20 year record. The four lidar records and one in situ record capture three background periods, which comprise ~40% of the measurements at these sites, with the post Pinatubo background period encompassing 20%. Thus, prior to Pinatubo, ~80% of the measurements were completed during volcanically perturbed periods.

[45] The disadvantages of such an effort is that no simple model of volcanic aerosol growth and decay can accurately capture all of the processes involved in the dispersal and removal of volcanic stratospheric aerosol as reflected in each of the various long-term measurements. This, however, does not preclude the application of an empirical model to remove the majority of the variance of the aerosol signal produced by volcanic eruptions. Such a model will be inherently tied to each measurement set and can only be applied to that measurement set. Application to a different set of measurements will use the same conceptual model but require a new set of parameters.

[46] The following considerations guided the choice of an empirical model to remove the volcanic influences: (1) The $1-2$ order of magnitude changes in aerosol signal from background to volcanic period suggest a log transform of the measurements to avoid excessive weighting of the volcanic period. (2) The roughly linear decay of any of the aerosol measures plotted in Figures 2 and 3, on a log scale, suggests a roughly exponential decay of volcanic aerosol. This assumption has some problems as background aerosol levels are approached, but is generally valid and has been used often [*Yue et al.*, 1991; *Rosen et al.*, 1994; *Osborn et al.*, 1995; *Deshler et al.*, 1997]. (3) Although the initial aerosol pulse from an eruption arrives fairly rapidly, it is not instantaneous, and the period of time leading to the peak aerosol signal requires some attention. (4) Cumulative effects of volcanic inputs and background sources are assumed to be additive. Deviations from exponential decay, assumed above, are consistent with this assumption. (5) The nature of the data is such that some variation in the measurements is fairly constant (measurement uncertainties), and some increases with scale (local natural variations following large volcanic eruptions). Variations that increase with aerosol signal appear during and following volcanic inputs. Figure 6a, displaying the Garmisch lidar measurements on a linear scale, illustrates this point. The variations which increase with integrated backscatter dominate the variance of the signal. Because these effects dominate, it is natural to use a log scale to display data as in Figures 1–4. (6) We assume there is a nonvolcanic, background, component to stratospheric aerosol which would exist in the absence of volcanic eruptions. Based on the data this assumption is reasonable, certainly more reasonable than assuming there is no background aerosol. Explicit inclusion of a term for baseline in equation (1) is also more consistent with the data than is exclusion of the term.

[47] The goal of the modeling exercise is to determine if the background aerosol level has changed, or remained constant, over the course of the measurements. Displays on log scales indicate the data are approximately lognormally distributed. Measurement error and perhaps some of the natural variation, however, exists at a fairly constant level and is approximately normally distributed. The true total ''error'' in the data is thus probably a convolution of normal and lognormal components, but, overall, the lognormal effects dominate and we use a lognormal model to remove volcanic signals.

[48] Based on these considerations the following empirical model is developed for log{Y(t)}, where Y(t) is a time dependent aerosol measurement from any of the long-term
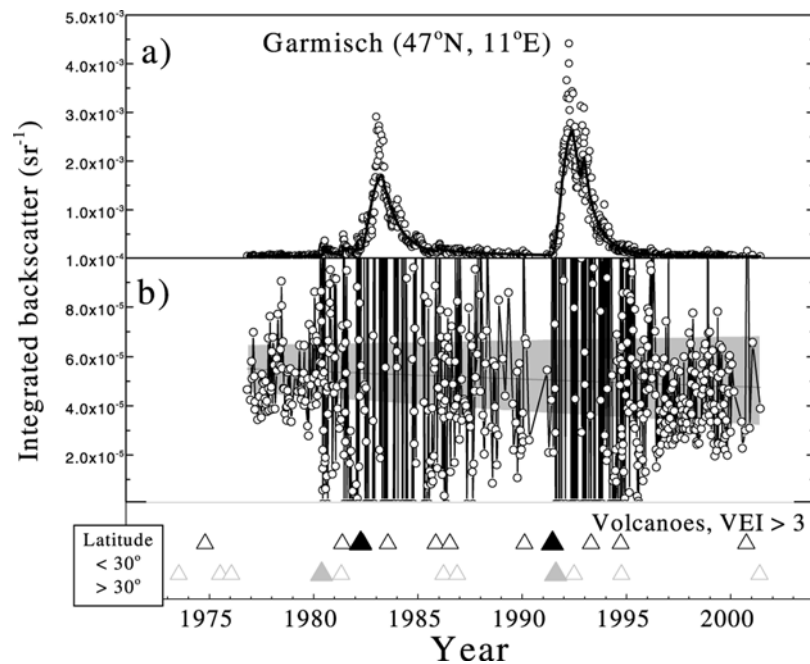
Figure 6. (a) Integrated backscatter (data points) from Garmisch, compared with the parametric model (solid line) for Garmisch, plotted on a linear scale. Compare the large variations near the peak of aerosol load for either El Chichón or Pinatubo with the variation of measurements near background. (b) Integrated backscatter for Garmisch with the modeled volcanic effects removed. Values become large and sometimes negative near the eruptions of El Chichón and Pinatubo due to the large natural variations around the volcanic model. Also shown are the mean and ±95% confidence limits for the modeled baseline and its trend. The times of the most significant volcanic eruptions during the period are indicated in Figure 6b with triangles, separated into those eruptions at latitudes less (upper symbol) and greater (lower symbol) than 30°. Eruptions with VEI of 5 (large solid symbol) and 4 (small open symbol) are shown. Names of the eruptions are listed in Table 1.

records. Plots of $\log\{Y(t)\}$ for the aerosol measurements under consideration are shown in Figures 2–4. The empirical model has the form

$$\log\{Y(t)\} = \log\left\{B\ \exp(\beta t) + \sum_1^N V_j(t)\right\} + \text{error.} \quad (1)$$

[49] The initial term $B \exp(\beta t)$ allows for an overall trend of the baseline, a value of $\beta = 0$ implies a constant baseline at B, whereas positive and negative values of β represent respectively growth and decline in background levels. The proposed model is thus based on a possibly changing baseline plus a chain of events added together over time. The number of measurable volcanic inputs over the observation period is determined by inspection from the data. Each volcanic input $V_j(t)$ consists of two parts, one for an initial, finite transition period during which aerosols are arriving, and the other for an open-ended period of decay. Exponential decay is assumed to be operative during both periods, although arrival dominates decay during the (usually brief) transition period, and only decay is present for the second period. In the second, more important period, starting at time τ_{jz}, the function is of simple form $P_j \exp(-\nu_j (t - \tau_{jz}))$ where P_j is the aerosol load at time τ_{jz} and ν_j is the volcano dependent exponential decay rate. The decay parameters ν_j are assumed positive, whereas β (the background growth or decay) can be positive or negative.

[50] The first period (transition) is less consequential but more complex. We assume that arrival of aerosols follows a positive continuous function $Q_j(t)$. These functions are modeled with three parameters: the time of appearance of volcanic aerosol at a site, τ_{ja}, the time when aerosols cease arriving, τ_{jz}, and the peak level of the wave over this interval, P_j, which may be shown to occur at τ_{jz}. Knowledge of event times puts a lower bound on each τ_{ja}. Assuming that the exact form of the wave is not critical, we use a truncated quadratic that is fixed at zero before τ_{ja} and after τ_{jz}. For time t between τ_{ja} and τ_{jz} the mean aerosol level is then $\int_{\tau_{ja}}^{\tau_{jz}} Q_j(t) \exp(-\nu_j(t - \tau_{ja}))dt$. The integral has a closed form that is perhaps unnecessarily complex, but it has the virtue of being parsimonious with respect to parameters and all parameters have physical interpretations.

[51] For N volcanoes the model has $4N + 2$ parameters, four for each volcano and two for the baseline. The chief drawback of this model is not, however, its dimension but rather the fact that conventional fitting is almost impossible to do exactly. The time limits τ_{ja} and τ_{jz} interject breaks in the smoothness of the function, and convergence is not feasible without unconventional optimization methods, or else careful monitoring and coaching of the process. For current purposes, a near optimal fit is satisfactory, because the primary purpose of the modeling is to allow volcanic inputs to be removed, leaving a baseline which can be
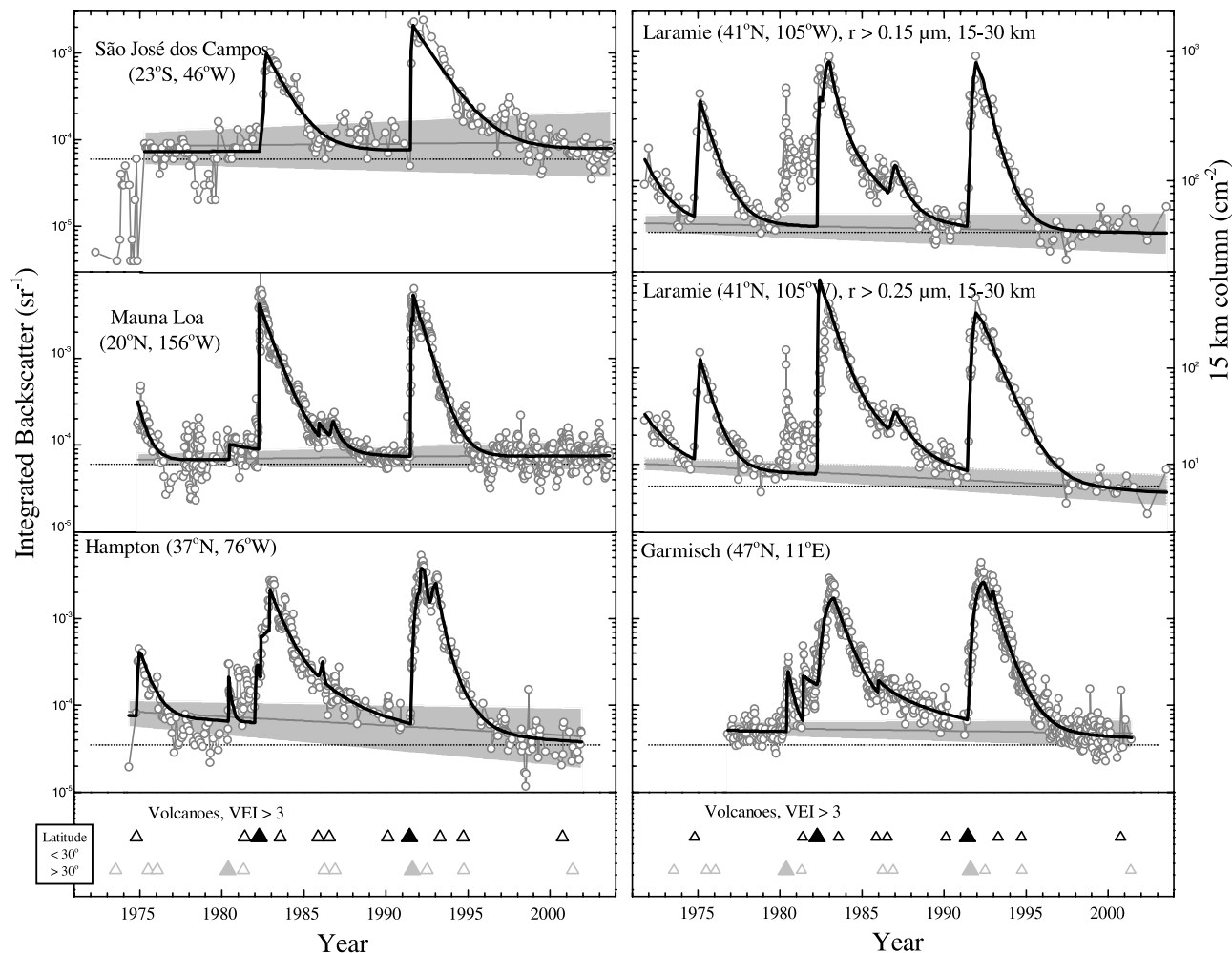
Figure 7. Integrated backscatter (data points) from São José dos Campos, Mauna Loa, Hampton and Garmisch lidar measurements, and integrated aerosol column (15–30 km) for particles with radius ≥0.15, 0.25 μm from Laramie compared with parametric model fits (solid lines) to the log of the measurements. The gray shaded areas provide the estimated background aerosol, with 95% confidence intervals, from the model. The time of volcanic eruptions with a VEI of 4 (open triangle) and 5 (solid triangle) are shown at the bottom divided into those eruptions at latitudes less than and greater than 30° of latitude, upper and lower symbols. The model was applied to the São José data beginning in 1975, and, as explained in the text, Mt. St. Helens was not included in the model for Laramie data.

assessed for trend, Figure 6b. The residuals are highly autocorrelated over time, and consequently simple linear regression trend analysis is not reliable in terms of inference. The degree of statistical significance is expected to be strongly inflated in these circumstances, so assessment of trend is done using a model that allows for first order autocorrelation. Data are unequally spaced in time, so analysis is performed using a one-dimensional spatial representation instead of a standard time series analysis [*Cressie*, 1993]. The advantages of this modeling exercise, over a simpler curve fitting exercise for every volcano in every measurement set, is that it provides a statistically objective approach to removing the volcanic signal, allows for autocorrelation, and provides an estimate of the confidence intervals in estimates of trends in the background aerosol.

[52] The optimization procedure uses a priori initial estimates for each parameter and then standard squared-error residual minimization to obtain the set of parameters providing the minimum in the residuals. Figure 6a presents the results obtained from a fit of the parametric model, equation (1), to the log of integrated backscatter from Garmisch. In this case 6 volcanic events were included so a 26 parameter model was used. The measurements compared to model estimates on a linear scale are shown in Figure 6a, while the aerosol signal with volcanic influences removed is shown in Figure 6b along with model estimates of the baseline trend with 95% confidence limits. The results of similar optimized fits to all of the lidar and the in situ measurements are shown in Figure 7, on a log scale to display variations during background periods. Also shown are model estimates of the baseline trend with 95% confidence limits and the times of volcanic eruptions with VEI ≥ 4. In all cases the model does a reasonable job of capturing the measurement variations through the volcanic perturbations. However, as apparent from Figure 7, not all

Table 2. Parameters Used in the Parametric Model Used to Estimate the Measurements From Each Long-Term Measurement Site[a]

Parameter		Laramie15	Laramie25	São José	Mauna Loa	Hampton	Garmisch
		15−30 km Column, cm^{-2}		Integrated Backscatter × 10^4, sr^{-1}			
Back-ground	B	47	10.2	0.83	0.68	0.85	0.55
	$\sigma(B)$	3.7	0.76	0.15	0.061	0.15	0.049
	β	−0.0056	−0.020	0.0039	0.0045	−0.024	−0.006
	$\sigma(\beta)$	0.0035	0.0035	0.0080	0.0039	0.0083	0.0042
Fuego	P	359	112	NA	2.9	3.7	NA
	$\sigma(P)$	34	12	NA	0.53	0.78	NA
	ν	1.11	1.48	NA	2.0	2.4	NA
	$\sigma(\nu)$	0.093	0.13	NA	0.34	0.47	NA
El Chichón	P	497	839	8.23	40.8	19	15.
	$\sigma(P)$	108	166	1.46	1.96	4.1	0.70
	ν	2.22	1.44	0.74	1.21	1.9	1.33
	$\sigma(\nu)$	0.76	0.22	0.096	0.037	0.79	0.13
Pinatubo	P	812	387	20.9	27.7	21.7	26
	$\sigma(P)$	45	22	4.0	43	1.76	1.05
	ν	1.26	0.976	0.70	1.45	4.62	3.2
	$\sigma(\nu)$	0.05	0.035	0.072	2.37	0.66	1.07

[a]The rate parameters, β, ν, have units of yr^{-1}. The standard errors of each parameter are indicated by σ. The 95% confidence intervals are given approximately by parameter ± 2σ. Only the background fit parameters incorporate autocorrelation in the estimates of standard errors.

volcanoes were included in the model for each site. Initially all volcanoes which appeared in the record were included. If convergence of the model was not achieved, then some of the smaller volcanoes were removed for that site and the

model rerun. This process was repeated until convergence was achieved. Thus, for example, Nevado del Ruiz and Nyamuragira were not included in the Sao Jose dos Campos model, whereas Mt. St. Helens was not included in the
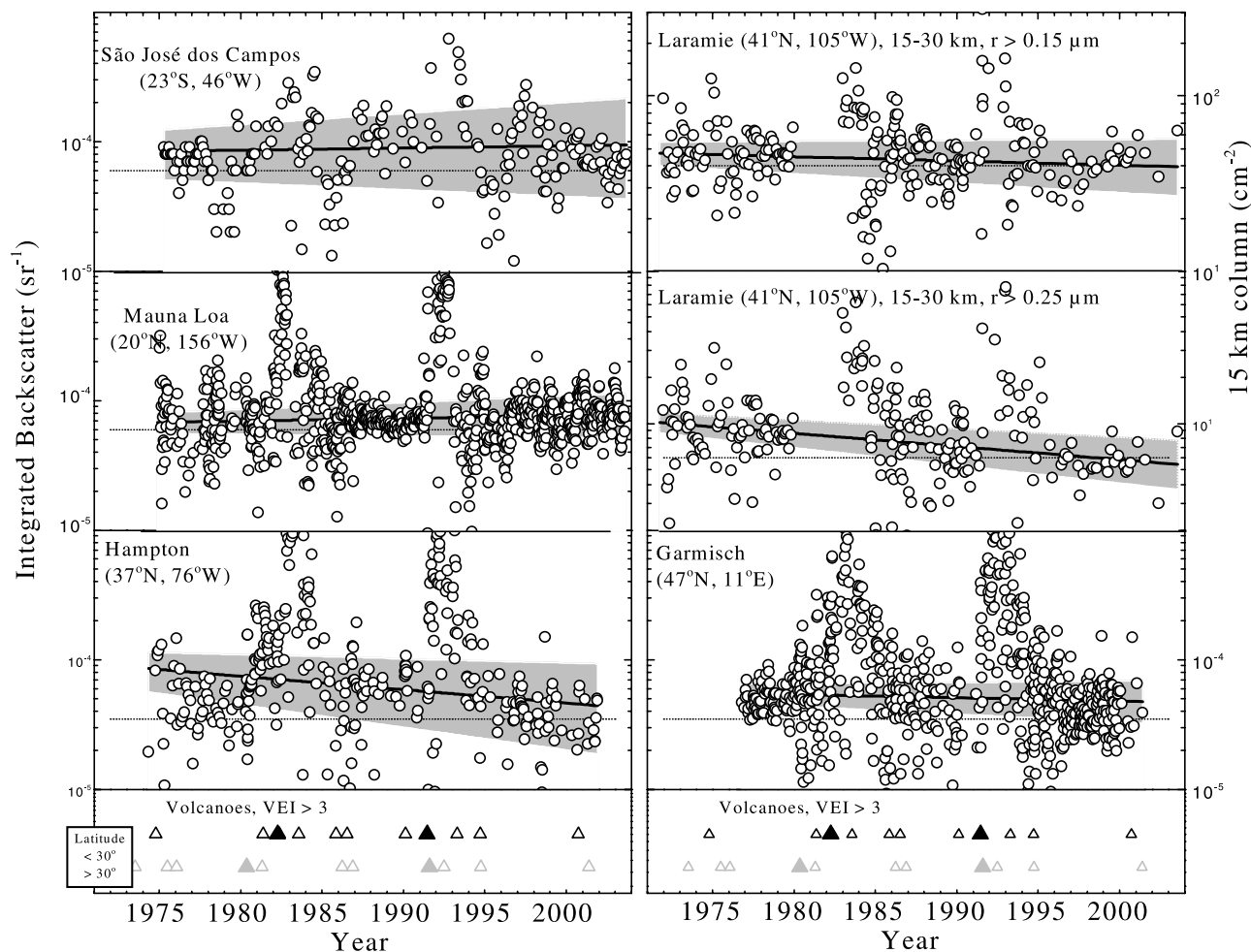

Figure 8. Same as Figure 7, except the data points are the measurements with the volcanic effect estimated from the model subtracted. The residuals for Laramie in 1980, following Mt. St. Helens, are off scale since Mt. St. Helens was not included in the model for Laramie.
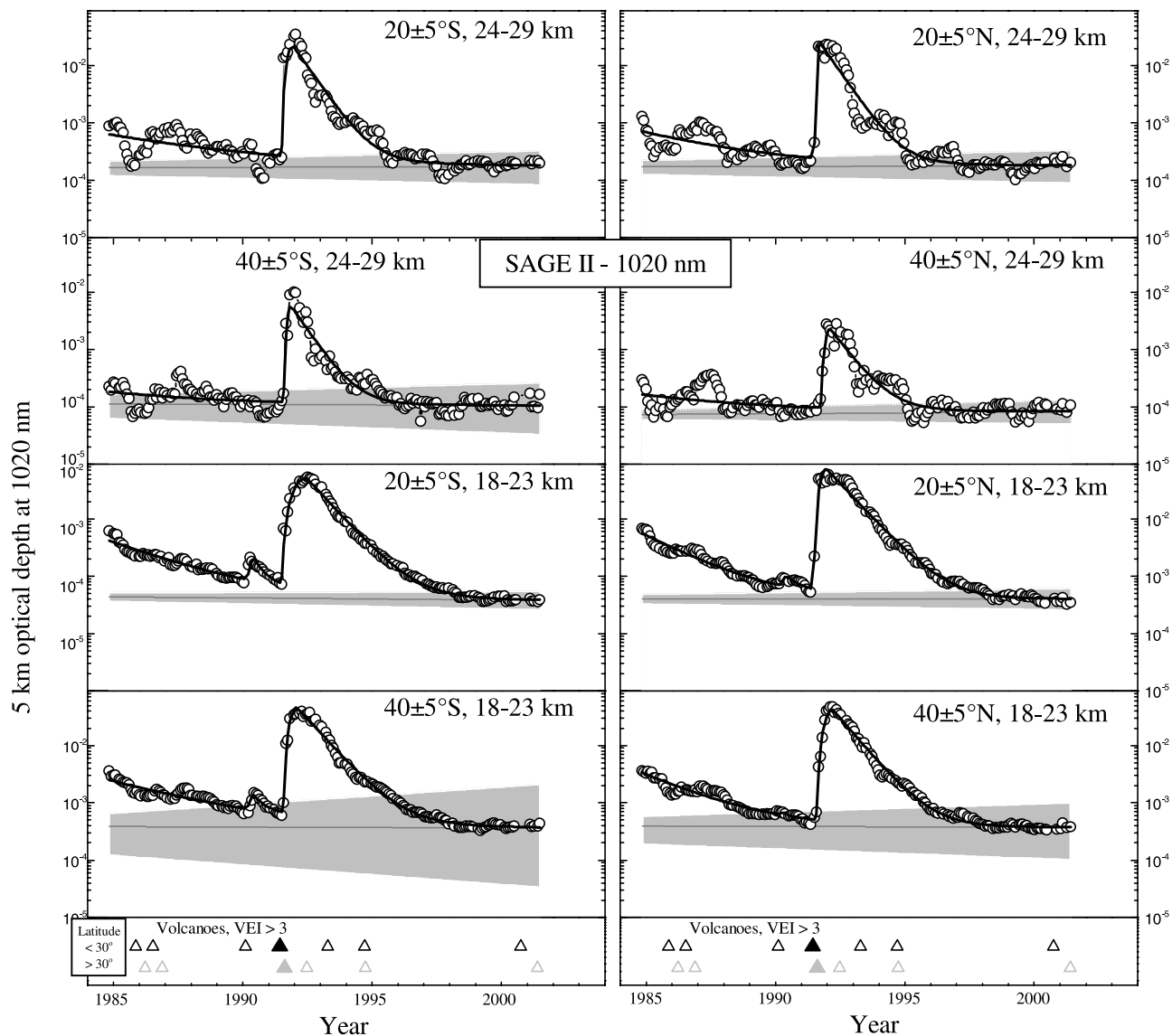
Figure 9. Optical depths integrated over two 5-kilometer altitude intervals for zonally averaged (±5°) SAGE II 1020 nm extinctions at a latitude of 20 and 40 ± 5°N/S, compared with parametric models fit to the data and with estimates of the baseline and trend for optical depth during background aerosol conditions. The estimated background is shown with ±95% confidence intervals as the gray shaded area. The time of volcanic eruptions with a VEI of 4 (open triangle) and 5 (solid triangle) are shown at the bottom divided into those eruptions at latitudes less than and greater than 30° of latitude.

Laramie record. Both the Laramie in situ data and Hampton lidar data were highly perturbed by Mt. St. Helens in comparison to other sites. This perturbation created difficulties in establishing a baseline prior to the eruption of El Chichón for the Hampton and Laramie data. Perhaps the proximity of this volcano and the increased sampling frequency at Laramie and Hampton contributed to these difficulties. For this analysis only elimination of these data from the Laramie record permitted the model to converge at reasonable levels. This extreme step was not taken for the Hampton data, but it is clear from Figure 7 that the minimum in the measurements prior to El Chichón, is not modeled correctly for Hampton.

[53] Table 2 provides the estimates of B, β, P_j and ν_j, along with their standard errors for each of the sites. The

95% confidence limits on any parameter are given approximately by plus and minus two standard errors of the mean. Time parameters τ_{ja} and τ_{jz} are omitted from the table. The measurements with modeled volcanic signal removed for the lidar and in situ records along with the baseline ± 95% confidence interval are shown in Figure 8.

[54] Based on Figures 7 and 8 and Table 2 the exponential change in the baseline, β, does not differ significantly from zero for the Garmisch, Mauna Loa, São José, and Laramie 0.15 μm records. Slight negative trends, ~2% yr^{-1}, are determined for the Hampton and Laramie 0.25 μm measurements. These results, suggesting a stable, or at most a slightly decreasing, stratospheric background aerosol, are consistent with the simpler analysis of background periods discussed in section 4.1. Only the Laramie 0.25 μm mea-

Table 3. Parameters Used to Model Zonal, ±5°, 5 km Optical Depths at 1020 nm From SAGE II[a]

Alt, km	Latitude, °	Background				El Chichón				Pinatubo			
		B	$\sigma(B)$	β	$\sigma(\beta)$	P	$\sigma(P)$	ν	$\sigma(\nu)$	P	$\sigma(P)$	ν	$\sigma(\nu)$
18–23	−50	3.00	0.15	0.0055	0.003	15.5	0.96	0.27	0.03	369.0	19.5	1.19	0.03
18–23	−40	3.86	2.32	−0.0039	0.037	21.4	2.12	0.31	0.05	459.5	22.0	1.15	0.03
18–23	−30	3.87	0.32	−0.0019	0.006	27.8	1.29	0.34	0.02	435.9	16.0	1.14	0.02
18–23	−20	4.36	0.37	−0.0083	0.006	37.9	1.64	0.40	0.02	512.3	18.3	1.14	0.02
18–23	−10	3.74	0.50	0.0014	0.009	60.6	3.09	0.44	0.02	1187.2	52.0	1.05	0.02
18–23	0	3.48	0.80	0.0064	0.016	93.5	7.17	0.53	0.03	1152.9	74.6	1.10	0.41
18–23	10	3.74	0.60	0.0043	0.011	82.5	5.37	0.56	0.03	1002.1	58.1	1.05	0.02
18–23	20	4.03	0.38	−0.0003	0.007	53.3	2.85	0.54	0.02	749.4	34.6	1.11	0.02
18–23	30	4.15	0.30	−0.0015	0.006	39.8	1.89	0.51	0.02	518.8	19.5	1.19	0.02
18–23	40	3.92	1.01	−0.0027	0.018	30.2	1.56	0.47	0.05	413.9	17.9	1.21	0.03
18–23	50	2.97	1.13	0.0082	0.025	21.7	1.42	0.41	0.06	287.3	16.2	1.18	0.04
24–29	−50	0.06	0.00	0.0009	0.009	0.1	0.00	0.00	0.01	2.3	0.4	2.97	0.27
24–29	−40	0.07	0.01	0.0002	0.009	0.1	0.01	0.00	0.01	1.8	0.3	2.75	0.35
24–29	−30	1.27	0.12	0.0008	0.009	1.6	0.30	0.23	0.06	88.0	11.4	1.49	0.10
24–29	−20	1.61	0.23	0.0028	0.011	4.9	0.60	0.24	0.03	235.0	30.3	1.34	0.07
24–29	−10	2.06	0.31	0.0008	0.012	10.9	0.91	0.25	0.02	484.3	47.1	1.33	0.05
24–29	0	2.22	0.37	0.0014	0.013	14.7	1.37	0.30	0.03	463.4	45.2	1.26	0.05
24–29	10	2.01	0.30	0.0043	0.012	11.3	1.14	0.32	0.03	338.9	37.5	1.36	0.06
24–29	20	1.73	0.24	0.0021	0.011	5.5	0.77	0.30	0.05	247.8	37.5	1.53	0.08
24–29	30	1.08	0.13	0.0029	0.011	2.1	0.37	0.27	0.06	72.6	10.2	1.44	0.10
24–29	40	0.74	0.07	0.0060	0.008	0.9	0.16	0.22	0.05	22.0	2.9	1.39	0.12
24–29	50	0.45	0.05	0.0043	0.010	0.5	0.06	0.07	0.02	10.1	1.4	1.35	0.14
30–35	−50	0.11	0.01	0.0000	0.005	0.0	0.02	0.56	1.04	1.7	0.2	2.66	0.27
30–35	−40	0.14	0.01	0.0044	0.005	0.0	0.02	0.44	0.39	1.8	0.3	2.68	0.33
30–35	−30	0.11	0.01	0.0005	0.011	0.1	0.01	0.01	0.01	5.0	0.9	12.86	2.98
30–35	−20	0.21	0.03	0.0017	0.013	0.2	0.03	0.03	0.02	19.6	5.6	11.88	2.12
30–35	−10	0.43	0.04	0.0065	0.009	0.4	0.14	0.46	0.18	10.1	1.9	1.62	0.20
30–35	0	0.45	0.04	0.0099	0.008	0.5	0.13	0.45	0.13	11.1	1.6	1.48	0.14
30–35	10	0.38	0.03	0.0054	0.008	0.3	0.08	0.29	0.10	5.2	0.6	1.50	0.20
30–35	20	0.29	0.03	0.0035	0.009	0.1	0.05	0.19	0.12	3.3	0.4	1.58	0.27
30–35	30	0.13	0.01	0.0199	0.009	0.1	0.02	0.15	0.06	1.4	0.2	1.62	0.32
30–35	40	0.09	0.01	0.0212	0.007	0.1	0.01	0.15	0.05	0.4	0.1	1.56	0.23
30–35	50	0.09	0.00	0.0065	0.005	0.0	0.01	0.22	0.36	0.3	0.0	1.69	0.24

[a]Optical depth ($\times 10^4$) and exponential change (yr^{-1}) are given for the baseline and the major impacts of El Chichón and Pinatubo along with their standard errors (σ). The 95% confidence intervals are given by parameter $\pm 2\sigma$.

surements result in a slight negative trend for both types of analyses. The simpler analysis of Hampton data suggests no trend, with perhaps a slight negative trend for Mauna Loa. For the Laramie 0.25 μm measurements the parametric model estimate of background aerosol decreasing at ∼2% yr^{-1} exceeds the ∼1% yr^{-1} estimated from the analysis of background periods. Errors in the measurements do not allow finer limits to be placed on possible changes.

[55] A similar model was applied to SAGE II satellite data. For this analysis the SAGE II extinctions were zonally averaged into ±5° latitude bins and optical depths calculated in three 5 km altitude intervals, 18–23, 24–29, and 30–35 km. The latitude bins were centered at 0, ±10, ±20, ±30, ±40, and ±50°. This subdivision of the SAGE II measurements provided 33 data sets for each of the four SAGE II extinction measurements. These data are less complex than the lidar and in situ data since the time period covered is only two thirds of the lidar and in situ data and volcanic eruptions were less frequent during this period. The number of volcanic events included in models of the SAGE II measurements varied from 3–4 depending on latitude. The tropical eruption of Kelut, a year prior to Pinatubo, did not affect the high latitude measurements. The analysis was completed for all 33 data sets for the 1020 nm extinction measurements since this is the most stable SAGE II aerosol measurement. These results are expected to apply equally as well to some of the other wavelengths; however,

care would be required if the shortest wavelength, 385 nm, was used. Time restraints prevented extending the investigation to other wavelengths.

[56] Figure 9 presents the results of parametric model fits to SAGE II 5 km optical depths for 4 latitude intervals and 2 altitude intervals. Table 3 provides the parameters which were obtained from the nonlinear least squares regression applied to the zonally-averaged SAGE II optical depths. Figure 10 provides the SAGE II measurements with the volcanic signal removed compared with the baseline estimates. Figure 10, as Figure 8, includes the removal of only the volcanic signal. Thus any changes in the background aerosol will appear in Figures 8 and 10. The results, Figure 10 and Table 3, are consistent with the ground-based lidar and balloonborne in situ measurements. The value of the exponential change for background aerosol, β, is not, statistically, significantly different than zero for the 20 year SAGE II measurement record. These results shown for SAGE II are indicative of similar analyses at ± 10, 30, and 50°.

[57] These results highlight the usefulness of this approach for trend analysis of the 20 years of SAGE II measurements. A simple comparison of the volcanically quiescent periods in the SAGE II measurements, Figure 4, would preclude such a conclusion. Figure 4 suggests either a decline in background stratospheric aerosol or background was not reached at most latitudes prior to the eruption of Pinatubo.
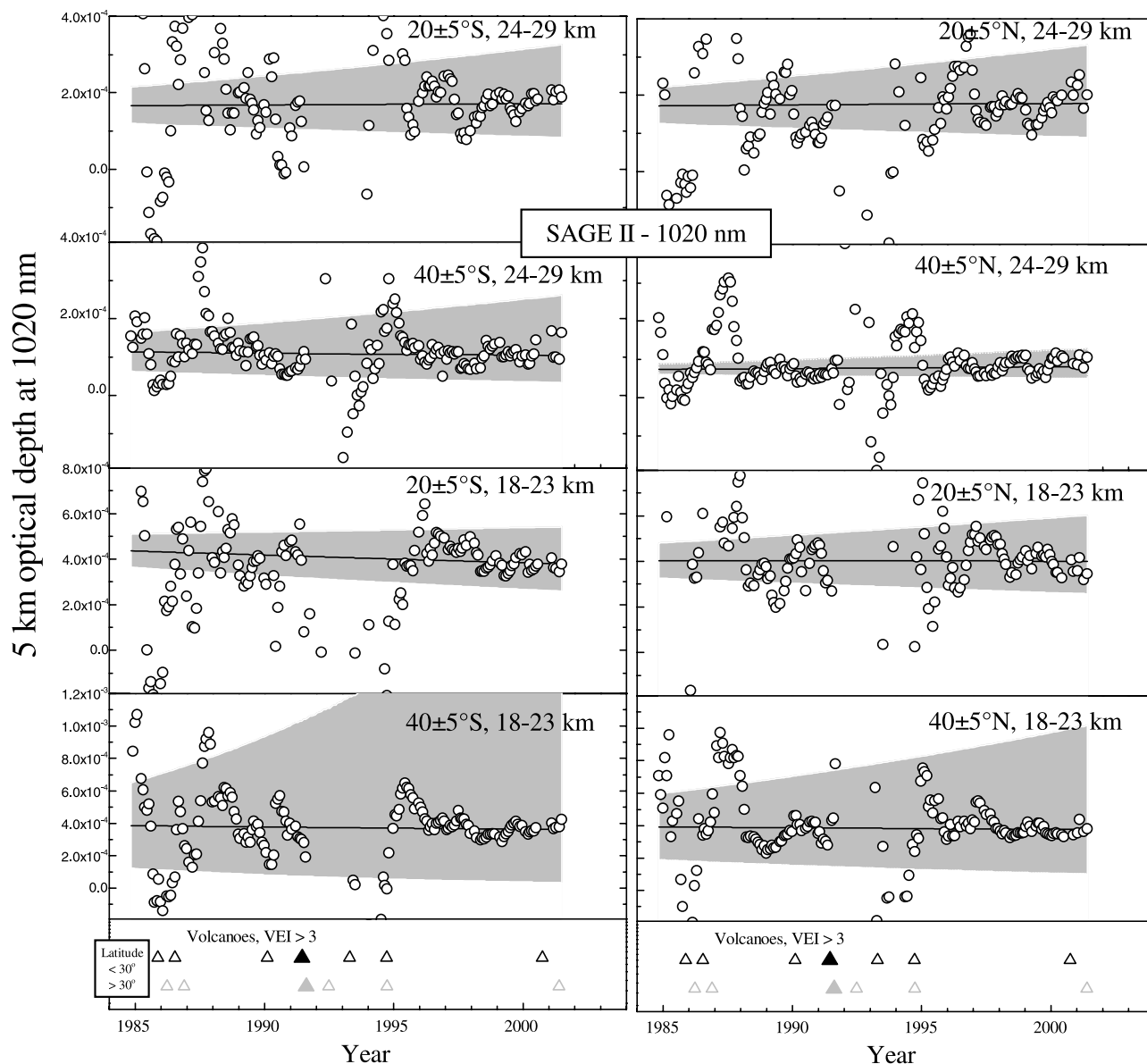
Figure 10. Same as Figure 9, except the data points are the measurements with the volcanic effect estimated from the model subtracted.

[58] Figure 11 summarizes the latitude distribution of the background exponential decay term, β (yr^{-1}), with 95% confidence intervals, for SAGE II 1020 nm 5 km optical depths at three altitudes, four lidar records, and in situ measurements at two sizes. For the lidar and in situ measurements estimates from both the analysis of background periods and the parametric model are shown. All data records are consistent in providing estimates for a trend in background aerosol which are not significantly different from zero, except for the Hampton lidar and Laramie 0.25 μm in situ measurements (negative trend) and two SAGE II zonal averages, 30–35 km, 30 and 40°N (positive trend). As mentioned earlier both the in situ data from Laramie and the Hampton lidar data were highly perturbed by Mt. St. Helens in comparison to other sites. Thus, while these data suggest, at a minimum, no long-term increase in background aerosol, they do not establish a long-term

decrease. The reason for the elevated values of β for SAGE II at these same latitudes is unknown.

5. Summary and Conclusions

[59] Understanding the nonvolcanic fraction of stratospheric aerosol has been one focus of stratospheric aerosol measurements since their inception over 40 years ago. Questions such as what are the source gases, how are they transported and transformed in the stratosphere, has there been an impact on natural background levels due to air traffic or other anthropogenic activities, and has the natural background aerosol changed over the course of measurements, have motivated measurements and analyses of background periods. Providing measurements to address these questions, however, has been difficult due to fairly active volcanism over the past 40 years, Table 1, with only the post
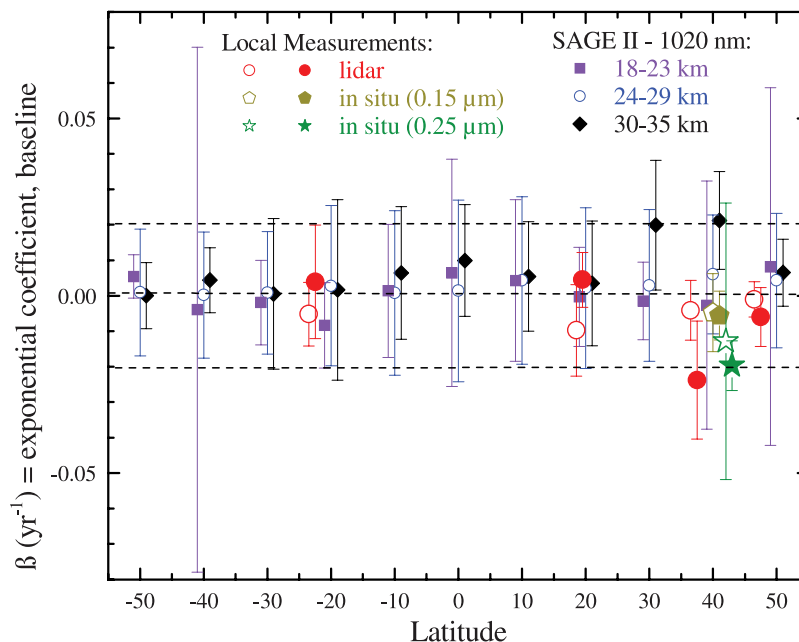
Figure 11. Exponential coefficient β (yr^{-1}) $\pm$ 95% confidence interval, as a function of latitude for (1) zonal averages ($\pm 5°$) of 5 km optical depths at 1020 nm from SAGE II for three altitude intervals, (2) integrated backscatter from São José dos Campos, Mauna Loa, Hampton, and Garmisch, and (3) 15–30 km column integrals of aerosol concentration for particles with radius $\geq$ 0.15 and 0.25 μm. For the lidar and in situ data the open symbol represents β based on the analysis of the three volcanically quiescent periods, while the solid symbol represents β obtained from the parametric model. In all cases the values of β are plotted around the central latitude for clarity and the error bars represent 95% confidence intervals.

Pinatubo period providing an interval allowing perhaps the first truly nonvolcanic aerosol measurements since regular measurements began in the early 1970s. Lidar measurements from 1977–1980 are comparable to the post Pinatubo period in the northern hemisphere, and perhaps lower than the post Pinatubo period in the southern hemisphere; however, the length of the post Pinatubo volcanically quiescent period far exceeds anything observed earlier. In addition in situ measurements were elevated from 1977–1979, reaching a minimum only after 1979. Thus, the post Pinatubo period provides our best opportunity to observe a stratosphere unperturbed by volcanic activity since long-term stratospheric aerosol measurements began. Comparing observations during the post Pinatubo period with predictions from global stratospheric aerosol models [e.g., *Weisenstein et al.*, 1997; *Timmreck*, 2001; *Pitari et al.*, 2002] will provide our best opportunity to assess the importance of COS and SO$_2$ in maintaining the background aerosol, and to assess the impact of changes in these sources gases.

[60] *Junge et al.* [1961] initiated stratospheric aerosol measurements in the late 1950s, which was at the end of a volcanically quiescent period. For this reason these measurements provided a baseline against which measurements in the 1970s and 1980s were compared. This provided the basis for early assessments of stratospheric aerosol which concluded that there had been an increase in the background aerosol on the order of 5–9% yr^{-1} [*Hofmann and Rosen*, 1980; *Sedlacek et al.*, 1983]. Now, with the benefit of minimal volcanism since Pinatubo, we can complete a definitive comparison with Junge's initial measurements, Figure 1. From this comparison we conclude that the stratospheric aerosol measurements which can be reliably used to assess trends in the nonvolcanic component of stratospheric aerosol began in the early 1970s. Earlier assessments of trends in nonvolcanic stratospheric aerosol, which included Junge's initial measurements, 1959–1960, were probably premature. Based on the stability of measurements following the decay of Pinatubo volcanic aerosol, we conclude that Junge's initial in situ measurements underestimated the size range or number concentration, or both, and thus these measurements cannot be reliably compared with the in situ record begun in 1971 and continued to the present. This interpretation is predicated on the assumption that the source gases for background stratospheric aerosol were comparatively stagnant over this period.

[61] Anthropogenic emissions of SO$_2$ increased 2% yr^{-1} from 1960–1990 and then decreased at about the same rate 1990–2000, Figure 2 [*van Aardenne et al.*, 2001]. Tropospheric COS captured in firn ice in Antarctica increased at a rate of 0.5% yr^{-1}, 1960–1980, remained relatively constant 1980–1990 and then decreased at 0.5% yr^{-1} since 1990 [*Montzka et al.*, 2004]. The extent to which these variations in tropospheric source gases directly influence background stratospheric aerosol is beyond the scope of this paper; however, a simple calculation assuming a linear response in stratospheric aerosol to these source gas changes, and fractional contributions to stratospheric aerosol of 35, 25 and 40% from COS, SO$_2$, and tropospheric sulfate aerosol [*Weisenstein et al.*, 1997; *Pitari et al.*, 2002], suggests

changes in stratospheric aerosol significantly less than the early estimates of increases in background aerosol.

[62] To provide an objective analysis of the stratospheric aerosol record since 1970 the statistical analysis of the 6 long-term stratospheric aerosol records (1 in situ, 4 lidars, 1 satellite) were approached in two ways. First, measurements limited to the three volcanically quiescent periods were compared using standard techniques. Second, an empirical model was developed to remove the volcanic signal from the long-term records and to investigate the "de-volcanized" measurements for trend.

[63] Comparison of measurements within the 3 volcanically quiescent periods, pre El Chichón, pre Pinatubo and post Pinatubo, were completed using the 1 in situ and 4 lidar records. In 3 of the 4 lidar records (Garmisch, Hampton, São José), and in the 0.25 μm in situ record, the pre-Pinatubo period is elevated compared to the other two periods. Simple linear regression over the three periods is controlled by the end points, pre El Chichón, post Pinatubo, and indicates either no change (Garmisch, Hampton, São José dos Campos, Laramie-0.15 μm) or a slight decrease in stratospheric aerosol (Mauna Loa, Laramie-0.25 μm). Problems with a simple linear regression are due to irregular temporal data and the high degree of autocorrelation. Including autocorrelation in the estimates decreases confidence in the estimates (increases standard errors), but does not change the conclusion that the majority of data indicate no trend in background stratospheric aerosol, 1970–2005. Two data sets suggest a slight negative trend, $-1 \pm 0.5\%/\mathrm{yr}^{-1}$, which is not statistically significant.

[64] A time and volcano dependent empirical model was fit to the long-term aerosol records to "de-volcanize" the data and thus analyze the entire data set for trend. Working in log space was a natural choice to treat errors during cases of high and low aerosol load equally. The empirical model also included a parameter to capture trends in the background aerosol. A standard squared-error residual minimization technique was employed to estimate the optimum parameters for the model for each measurement and each site. This included 4 lidar data sets, 2 in situ data sets (two aerosol sizes) and 33 SAGE II data sets (optical depths at 1020 nm at three altitude and eleven latitude intervals). These analyses allowed for first order autocorrelation and used a one-dimensional spatial representation to account for the temporally disparate sampling intervals. As with the simpler comparison of background periods the autocorrelation increases the standard errors of the trends but does not change the magnitude. For 31 of 33 SAGE II data sets, 3 of 4 lidar records, and in situ measurements at 0.15 μm the analyses suggest no long-term trend in stratospheric aerosol. For one lidar site (Hampton) and in situ measurements at 0.25 μm, the results suggest a weak negative trend, on the order of $-2 \pm 0.5\%\ \mathrm{yr}^{-1}$. Both these estimates suffer from difficulties introduced by Mt. St. Helens, and a comparison of the model with the data suggests problems in representing properly the measurements prior to El Chichón. In contrast to these two estimates of a negative trend, two SAGE II data sets (30–35 km, 30° and 40°N) suggest a positive trend of the same magnitude, 2% yr^{-1}.

[65] The overall conclusion from both the simple analysis of quiescent periods and the empirical model fit to the measurements is that background stratospheric aerosol has not displayed a long-term trend over the period 1970–2005. This conclusion is supported by 94% of the satellite data analyzed, 75% of the lidar data, and 50% of the in situ data. The conclusion from the remaining data is not compelling. In addition to this result from statistical analyses, the long volcanically quiescent period following Pinatubo allows each record to be inspected for trend over a period of 5 to 8 years, and all are consistent in showing no significant change over this latter period.

[66] The statistical analyses were completed on altitude/latitude integrals of the measurements, precluding establishing, or ruling out, long-term changes in microphysical properties of background stratospheric aerosol. Some information concerning the long-term tendency of aerosol size distributions is available by comparing altitude integrals of the two sizes, r > 0.15, 0.25 μm, measured. Some differences were observed, but these were not statistically significant.

References

Angell, J. K. (1993), Comparisons of stratospheric warming following Agung, El Chichón, and Pinatubo volcanic eruptions, *Geophys. Res. Lett.*, *20*, 715–718.

Angell, J. K., J. Korshover, and W. G. Planet (1985), Ground-based and satellite evidence for a pronounced total-ozone minimum in early 1983 and responsible atmospheric layers, *Mon. Weather Rev.*, *113*, 641–646.

Barnes, J. E., and D. J. Hofmann (1997), Lidar measurements of stratospheric aerosol over Mauna Loa, *Geophys. Res. Lett.*, *24*, 1923–1926.

Barnes, J. E., and D. J. Hofmann (2001), Variability in the stratospheric background aerosol over Mauna Loa observatory, *Geophys. Res. Lett.*, *28*, 2895–2898.

Carn, S. A., A. J. Krueger, G. J. S. Bluth, S. J. Schaeffer, N. A. Krotkov, I. M. Watson, and S. Datta (2003), Volcanic eruption detection by the Total Ozone Mapping Spectrometer (TOMS) instruments: A 22-year record of sulphur dioxide and ash emissions, in *Volcanic Degassing*, edited by C. Oppenheimer, D. M. Pyle, and J. Barclay, *Geol. Soc. London Spec. Publ.*, *213*, 177–202.

Chagnon, C. W., and C. E. Junge (1961), The vertical distribution of submicron particles in the stratosphere, *J. Meteorol.*, *18*, 746–752.

Chu, W. P., M. P. McCormick, J. Lenoble, C. Brogniez, and P. Pruvost (1989), SAGE II inversion algorithm, *J. Geophys. Res.*, *94*, 8339–8351.

Clemesha, B. R., and D. M. Simonich (1978), Stratospheric dust measurements 1970–1977, *J. Geophys. Res.*, *83*, 2403–2408.

Cressie, N. A. C. (1993), *Statistics for Spatial Data*, John Wiley, Hoboken, N. J.

Crutzen, P. J. (1970), The influence of nitrogen oxide on the atmospheric ozone content, *Q. J. R. Meteorol. Soc.*, *96*, 320–327.

DeFoor, J. E., E. Robinson, and S. Ryan (1992), Early lidar measurements of the June 1991 Pinatubo eruption plume at Manua Loa Observatory, Hawaii, *Geophys. Res. Lett.*, *19*, 187–190.

Deshler, T., and R. Anderson-Sprecher (2006), Investigating trends in the nonvolcanic component of stratospheric aerosol over the period 1971–2004, in *SPARC Assessment of Stratospheric Aerosol Properties*, edited by L. Thomason and T. Peter, chap. 5, in press.

Deshler, T., B. J. Johnson, and W. R. Rozier (1993), Balloonborne measurements of Pinatubo aerosol during 1991 and 1992 at 41°N, vertical profiles, size distribution, and volatility, *Geophys. Res. Lett.*, *20*, 1435–1438.

Deshler, T., B. J. Johnson, D. J. Hofmann, and B. Nardi (1996), Correlations between ozone loss and volcanic aerosol at latitudes below 14 km over McMurdo Station, Antarctica, *Geophys. Res. Lett.*, *23*, 2931–2934.

Deshler, T., J. B. Liley, G. Bodeker, W. A. Matthews, and D. J. Hofmann (1997), Stratospheric aerosol following Pinatubo, comparison of the

north and south midlatitudes using in situ measurements, *Adv. Space Res.*, 20, 2057–2061.

Deshler, T., M. E. Hervig, D. J. Hofmann, J. M. Rosen, and J. B. Liley (2003), Thirty years of in situ stratospheric aerosol size distribution measurements from Laramie, Wyoming (41°N), using balloon-borne instruments, *J. Geophys. Res.*, 108(D5), 4167, doi:10.1029/2002JD002514.

Dutton, E. G., and J. R. Christy (1992), Solar radiative forcing at selected locations and evidence for global lower tropospheric cooling following the eruptions of El Chichón and Pinatubo, *Geophys. Res. Lett.*, 19, 2313–2316.

Fahey, D. W., et al. (1993), In situ measurements constraining the role of sulphate aerosols in midlatitude ozone depletion, *Nature*, 363, 509–514.

Fernald, F. G., and B. G. Schuster (1977), Wintertime 1973 airborne lidar measurements of stratospheric aerosols, *J. Geophys. Res.*, 82, 433–437.

Fiocco, G., and G. Grams (1964), Observation of aerosol layer of 20 km by optical radar, *J. Atmos. Sci.*, 21, 323–324.

Fuller, W. H., Jr., M. T. Osborn, and W. H. Hunt (1988), 48-inch lidar aerosol measurements taken at the Langley Research Center: May 1974 to December 1987, *NASA RP, 1209*.

Gleason, J. F., et al. (1993), Record low global ozone in 1992, *Science*, 260, 523–526.

Gruner, P., and H. Kleinert (1927), Die Dämmerungserscheinungen, *Probl. Kosm. Phys.*, 10, 1–113.

Halmer, M. M., H.-U. Schmincke, and H.-F. Graf (2002), The annual volcanic gas input into the atmosphere, in particular into the stratosphere: A global data set for the past 100 years, *J. Volcanol. Geotherm. Res.*, 115, 511–528.

Hansen, J., A. Lacis, R. Ruedy, and K. Sato (1992), Potential climate impact of Mount Pinatubo eruption, *Geophys. Res. Lett.*, 19, 215–218.

Hayashida, S., and M. Horikawa (2001), Anti-correlation between stratospheric aerosol extinction and the Ångström parameter from multiple wavelength measurements with SAGE II - A characteristic of the decay period following major volcanic eruptions, *Geophys. Res. Lett.*, 28, 4063–4066.

Hervig, M. E., and T. Deshler (2002), Evaluation of aerosol measurements from SAGE II, HALOE, and balloonborne optical particle counters, *J. Geophys. Res.*, 107(D3), 4031, doi:10.1029/2001JD000703.

Hicks, B. B., R. S. Artz, T. P. Meyers, and R. P. Hosker Jr. (2002), Trends in eastern U.S. sulfur air quality from the Atmospheric Integrated Research Monitoring Network, *J. Geophys. Res.*, 107(D12), 4143, doi:10.1029/2000JD000165.

Hofmann, D. J. (1990), Increase in the stratospheric background sulfuric acid aerosol mass in the past 10 years, *Science*, 248, 996–1000.

Hofmann, D. J., and T. Deshler (1991), Stratospheric cloud observations during formation of the Antarctic ozone hole in 1989, *J. Geophys. Res.*, 96, 2897–2912.

Hofmann, D. J., and J. M. Rosen (1980), Stratospheric sulfuric acid layer: Evidence for an anthropogenic component, *Science*, 208, 1368–1370.

Hofmann, D. J., and J. M. Rosen (1981), On the background stratospheric aerosol layer, *J. Atmos. Sci.*, 38, 168–181.

Hofmann, D. J., and S. Solomon (1989), Ozone destruction through heterogeneous chemistry following the eruption of El Chichón, *J. Geophys. Res.*, 94, 5029–5041.

Hofmann, D. J., J. M. Rosen, T. J. Pepin, and R. G. Pinnick (1975), Stratospheric aerosol measurements, I, Time variations at northern midlatitudes, *J. Atmos. Sci.*, 32, 1446–1456.

Hofmann, D. J., J. Barnes, E. Dutton, T. Deshler, H. Jäger, R. Keen, and M. Osborn (2003), Surface-based observations of volcanic emissions to the stratosphere, in *Volcanism and the Earth's Atmosphere, Geophys. Monogr. Ser.*, vol. 139, edited by A. Robock and C. Oppenheimer, pp. 57–73, AGU, Washington, D. C.

Jäger, H. (2005), Long-term record of lidar observations of the stratospheric aerosol layer at Garmisch-Partenkirchen, *J. Geophys. Res.*, 110, D08106, doi:10.1029/2004JD005506.

Jäger, H., and D. J. Hofmann (1991), Midlatidude lidar backscatter to mass, area, and extinction conversion model based on in situ aerosol measurements from 1980 to 1987, *Appl. Opt.*, 30, 127–138.

Jäger, H., and K. Wege (1990), Stratospheric ozone depletion at northern midlatitudes after major volcanic eruptions, *J. Atmos. Chem.*, 10, 273–287.

Johnston, P.V., and R. L. McKenzie (1989), NO_2 observations at 45°S during the decreasing phase of solar cycle 21, from 1980 to 1987, *J. Geophys. Res.*, 94, 3473–3486.

Johnston, P. V., R. L. McKenzie, J. G. Keys, and W. A. Matthews (1992), Observations of depleted stratospheric NO_2 following the Pinatubo volcanic eruption., *Geophys. Res. Lett.*, 19, 211–213.

Junge, C. E., and J. E. Manson (1961), Stratospheric aerosol studies, *J. Geophys. Res.*, 66, 2163–2182.

Junge, C. E., C. W. Changnon, and J. E. Manson (1961), Stratospheric aerosols, *Meteorol*, 18, 81–108.

Kley, D., J. M. Russell III, and C. Phillips (2000), SPARC assessment of upper tropospheric and stratospheric water vapour, *Rep. 113*, World Clim. Res. Programme.

Labitzke, K., and M. P. McCormick (1992), Stratospheric temperature increases due to Pinatubo aerosols, *Geophys. Res. Lett.*, 19, 207–210.

Lee, R. L., and J. Hernandez-Andres (2003), Measuring and modeling twilight's purple light, *Appl. Opt.*, 42, 445–457.

Manabe, S., and R. T. Wetherald (1967), Thermal equilibrium of the atmosphere with a given distribution of relative humidity, *J. Atmos. Sci.*, 24, 241.

Mauldin, L. E., N. H. Zaun, M. P. McCormick, J. H. Guy, and W. R. Vaughn (1985), Stratospheric Aerosol and Gas Experiment II instrument: A functional description, *Opt. Eng.*, 24, 307–312.

McCormick, M. P., P. Hamill, T. J. Pepin, W. P. Chu, T. J. Swissler, and L. R. McMaster (1979), Satellite studies of the stratospheric aerosol, *Bull. Am. Meteorol. Soc.*, 60, 1038–1046.

McCormick, M. P., et al. (1981), High-latitude stratospheric aerosols measured by the SAM II satellite system in 1978 and 1979, *Science*, 214, 328–331.

McCormick, M. P., L. W. Thomason, and C. R. Trepte (1995), Atmospheric effects of the Mt. Pinatubo Eruption, *Nature*, 373, 399.

Montzka, S. A., M. Aydin, M. Battle, J. H. Butler, E. S. Saltzman, B. D. Hall, A. D. Clarke, D. Mondeel, and J. W. Elkins (2004), A 350-year atmospheric history for carbonyl sulfide inferred from Antarctic firn air and air trapped in ice, *J. Geophys. Res.*, 109, D22302, doi:10.1029/2004JD004686.

Mozurkiewicz, M., and J. G. Calvert (1988), Reaction probability of N_2O_5 on aqueous aerosols, *J. Geophys. Res.*, 93, 15,889–15,896.

Nedoluha, S., et al. (2004), Long-term variations in water vapor and their effect on ozone, paper presented at Quadrenniel Ozone Symposium, Kos, Greece, June .

Newhall, C. G., and S. Self (1982), The Volcanic Explosivity Index (VEI): An estimate of explosive magnitude for historical volcanism, *J. Geophys. Res.*, 87, 1231–1238.

Oberbeck, V. R., J. M. Libingston, P. B. Russell, R. F. Pueschell, J. M. Rosen, M. T. Osborn, M. A. Kritz, K. G. Snetsinger, and G. V. Ferry (1989), SAGE II aerosol validation: Selected altitude measurements, including particle micromeasurements, *J. Geophys. Res.*, 94, 8367–8380.

Oltmans, S. J., and D. J. Hofmann (1995), Increases in lower-stratospheric water vapor at a midlatitude northern hemisphere site from 1981 to 1994, *Nature*, 374, 146–149.

Osborn, M. T., J. M. Rosen, M. P. McCormick, P. Wang, J. M. Livingstion, and T. J. Swissler (1989), SAGE II aerosol correlative observations: Profile measurements, *J. Geophys. Res.*, 94, 8353–8366.

Osborn, M. T., R. J. DeCoursey, C. R. Trepte, D. M. Winder, and D. C. Woods (1995), Evolution of the Pinatubo volcanic cloud over Hampton, Virginia, *Geophys. Res. Lett.*, 22, 1101–1104.

Pepin, T. J., M. P. McCormick, W. P. Chu, F. Simon, T. J. Swissler, R. R. Adams, K. R. Crumbly, and W. H. Fuller Jr. (1977), Stratospheric aerosol measurements, *NASA Spec. Publ.*, SP-421, 127–136.

Pinnick, R. G., and D. J. Hofmann (1973), Efficiency of light-scattering aerosol particle counters, *Appl. Opt.*, 12, 2593–2597.

Pitari, G., E. Mancini, V. Rizi, and D. T. Shindell (2002), Impact of future climate and emission changes on stratospheric aerosols and ozone, *J. Atmos. Sci.*, 59, 414–440.

Pollack, J. B., O. B. Toon, C. Sagan, A. Summers, B. Baldwin, and W. V. Camp (1976), Volcanic explosions and climate change: A theoretical assessment, *J. Geophys. Res.*, 81, 1071–1083.

Poole, L. R., and M. C. Pitts (1994), Polar stratospheric cloud climatology based on Stratospheric Aerosol Measurement II observations from 1978 to 1989, *J. Geophys. Res.*, 99, 13,083–13,089.

Prather, M. J. (1992), Catastrophic loss of stratospheric ozone in dense volcanic clouds, *J. Geophys. Res.*, 97, 10,187–10,191.

Ramaswamy, V., et al. (2001), Stratospheric temperature trends: Observations and model simulations, *Rev. Geophys.*, 39, 71–122.

Reiter, R., H. Jäger, W. Carnuth, and W. Funk (1979), The stratospheric aerosol layer observed by lidar since October 1976: A contribution to the problem of hemispheric climate, *Arch. Met. Geoph. Biokl., Ser. B*, 27, 121–149.

Robock, A. (1981), The Mount St. Helens volcanic eruption of 18 May 1980: Minimal climatic effect, *Science*, 212, 1383–1384.

Rosen, J. M. (1964), The vertical distribution of dust to 30 km, *J. Geophys. Res.*, 69, 4673–4676.

Rosen, J. M., N. T. Kjome, R. L. McKenzie, and J. B. Liley (1994), Decay of Mount Pinatubo aerosol at midlatitudes in the northern and southern hemispheres, *J. Geophys. Res.*, 99, 25,733–25,739.

Rowland, F. S., H. Sato, H. Khwaja, and S. M. Elliott (1986), The hydrolysis of chlorine nitrate and its possible atmospheric significance, *J. Phys. Chem.*, 90, 1985–1988.

Russell, P. B., and D. Hake Jr. (1977), The post-Fuego stratospheric aerosol: Lidar measurements, with radiative and thermal implications, *J. Atmos. Sci.*, *34*, 163–177.

Russell, P. B., and M. P. McCormick (1989), SAGE II aerosol data validation and initial data use: An introduction and overview, *J. Geophys. Res.*, *94*, 8335–8338.

Russell, P. B., et al. (1981), Satellite and correlative measurements of the stratospheric aerosol. II: Comparison of measurements made by SAM II, dustsondes, and an airborne lidar, *J. Atmos. Sci.*, *38*, 1296–1312.

Russell, P. B., M. P. McCormick, T. J. Swissler, J. M. Rosen, D. J. Hofmann, and L. R. McMaster (1984), Satellite and correlative measurements of the stratospheric aerosol. III: Comparison of measurements made by SAM II, SAGE, dustsondes, filters, impactors, and lidar, *J. Atmos. Sci.*, *41*, 1792–1800.

Russell, P. B., et al. (1993), Pinatubo and pre-Pinatubo optical-depth spectra: Mauna Loa measurements, comparisons, inferred particle size distributions, radiative effects, and relationship to lidar data, *J. Geophys. Res.*, *98*, 22,969–22,985.

Sato, M., J. E. Hansen, M. P. McCormick, and J. B. Pollack (1993), Stratospheric aerosol optical depths, 1850–1990, *J. Geophys. Res.*, *98*, 22,987–22,994.

Schnetzler, C. C., G. J. S. Bluth, A. J. Krueger, and L. S. Walter (1997), A proposed volcanic sulfur dioxide index (VSI), *J. Geophys. Res.*, *102*(B9), 20,087–20,092.

Sedlacek, W. A., E. J. Mroz, A. I. Lazrus, and B. W. Gandrud (1983), A decade of stratospheric sulfate measurements compared with observations of volcanic eruptions, *J. Geophys. Res.*, *88*, 3741–3776.

Simkin, T., and L. Siebert (1994), *Volcanoes of the World: A Regional Directory, Gazeteer, and Chronology of Volcanism During the Last 10,000 Years*, 349 pp., Geosci.

Simonich, D. M., and B. R. Clemesha (1989), The decay of the El Chichon aerosol cloud at 23 degrees south, *J. Geophys. Res.*, *94*, 12,803–12,806.

Simonich, D. M., and B. R. Clemesha (1997), A history of aerosol measurements at São José dos Campos, Brazil (23 S, 46 W) from 1972 to 1995, in *Advances in Atmospheric Remote Sensing With Lidar - Selected Papers of the 18th International Laser Radar Conference*, pp. 481–484, Springer, New York.

Solomon, S. (1999), Stratospheric ozone depletion: A review of concepts and theory, *Rev. Geophys.*, *37*, 275–316.

Solomon, S., R. R. Garcia, F. S. Rowland, and D. J. Wuebbles (1986), On the depletion of Antarctic ozone, *Nature*, *321*, 755–758.

Solomon, S., R. W. Portmann, R. R. Garcia, L. W. Thomason, L. R. Poole, and M. P. McCormick (1996), The role of aerosol variations in anthropogenic ozone depletion at northern midlatitudes, *J. Geophys. Res.*, *101*, 6713–6727.

Steele, H. M., and P. Hamill (1981), Effect of temperature and humidity on the growth and optical properties of sulfuric acid-water droplets in the stratosphere, *J. Aerosol Sci.*, *12*, 517–528.

Stothers, R. B. (1996), Major optical depth perturbations to the stratosphere from volcanic eruptions: Pyrheliometric period, 1881–1960, *J. Geophys. Res.*, *101*, 3901–3920.

Thomason, L. W., and S. P. Burton (2006), SAGE II stratospheric aerosol extinction measurements in the lower tropical stratosphere at near nonvolcanic levels, *J. Atmos. Chem. Phys. Discuss.*, in press.

Thomason, L. W., G. S. Kent, C. R. Trepte, and L. R. Poole (1997a), A comparison of the stratospheric aerosol background periods of 1979 and 1989–1991, *J. Geophys. Res.*, *102*, 3611–3616.

Thomason, L. W., L. R. Poole, and T. Deshler (1997b), A global climatology of stratospheric aerosol surface area density deduced from stratospheric aerosol and gas experiment II measurements: 1984–1994, *J. Geophys. Res.*, *102*, 8967–8976.

Timmreck, C. (2001), Three-dimensional simulation of stratospheric background aerosol: First results of a multiannual general circulation model simulation, *J. Geophys. Res.*, *106*, 28,313–28,332.

Tolbert, M. A., M. J. Rossi, and D. M. Golden (1988), Heterogeneous interactions of chlorine nitrate hydrogen chloride and nitric acid with sulfuric acid surfaces at stratospheric temperatures, *Geophys. Res. Lett.*, *15*, 847–850.

van Aardenne, J. A., F. J. Dentener, J. G. J. Olivier, C. G. M. Klein Goldewijk, and J. Lelieveld (2001), A $1° \times 1°$ resolution data set of historical anthropogenic trace gas emissions for the period 1890–1990, *Global Biogeochem. Cycles*, *15*, 909–928.

Weisenstein, D. K., and S. Bekki (2006), Stratospheric aerosol modeling, in *SPARC Assessment of Stratospheric Aerosol Properties*, edited by L. Thomason and T. Peter, chap. 6, in press.

Weisenstein, D. K., G. K. Yue, M. K. W. Ko, N. D. Sze, J. M. Rodriguez, and C. J. Scott (1997), A two-dimensional model of sulfur species and aerosol, *J. Geophys. Res.*, *102*, 13,019–13,035.

Wennberg, P. O., et al. (1994), Removal of stratospheric O_3 by radicals: In situ measurements, of OH, HO_2, NO, NO_2, ClO, and BrO, *Science*, *266*, 398–404.

Woods, D. C., M. T. Osborn, D. M. Winker, R. J. DeCoursey, and O. Youngbluth (1994), 48-inch lidar aerosol measurements taken at the Langley Research Center: July 1991 to December 1992, *NASA RP*, *1334*.

Yue, G. K., M. P. McCormick, and E.-W. Chiou (1991), Stratospheric aerosol optical depth observed by the SAGE II experiment: Decay of the El Chichón and Ruiz volcanic perturbations, *J. Geophys. Res.*, *96*, 5209–5219.

————————————

R. Anderson-Sprecher, Department of Statistics, University of Wyoming, Laramie, WY 82071, USA.

J. Barnes and D. J. Hofmann, National Oceanic and Atmospheric Administration, Boulder, CO 80305, USA.

B. Clemesha and D. Simonich, Instituto Nacional de Pesquisas Espaciais, S. J. dos Campos 12227-010, Brazil.

T. Deshler, Department of Atmospheric Science, University of Wyoming, Laramie, WY 82071, USA. (deshler@uwyo.edu)

S. Godin-Beekmann, Service d'Aéronomie, CNRS, Institut Pierre Simon Laplace, Jussieu F-75252, France.

R. G. Grainger, Atmospheric, Oceanic, and Planetary Physics, Oxford University, Oxford OX1 3PU, UK.

H. Jäger, Institut für Meteorologie und Klimaforschung, Atmosphärische Umweltforschung (IMK-IFU), Forschungszentrum Karlsruhe GmbH, Garmisch-Partenkirchen D-82467, Germany.

M. Osborn, NASA Langley Research Center, Hampton, VA 23666, USA.